Recent developments in the use of heterogeneous semiconductor photocatalyst based materials for a visible-light-inducedwater-splitting system-a brief review

著者	Arunachalam Prabhakarn, Nagai Keiji, Amer Mabrook S., Ghanem Mohamed A., Ramalingam Rajabathar Jothi, Al-Mayouf Abdullah M.
著者別表示	長井 圭治
journal or publication title	Catalysts
volume	11
number	2
page range	160
year	2021-01-25
URL	http://hdl.handle.net/2297/00067090

doi: 10.3390/catal11020160

catalysts

MDPI

Review

Recent Developments in the Use of Heterogeneous Semiconductor Photocatalyst Based Materials for a Visible-Light-Induced Water-Splitting System—A Brief Review

Prabhakarn Arunachalam [1,2,*], Keiji Nagai [3], Mabrook S. Amer [1,2,4], Mohamed A. Ghanem [1,2], Rajabathar Jothi Ramalingam [2] and Abdullah M. Al-Mayouf [1,2,4]

1 Electrochemical Sciences Research, Chemistry Department, College of Science, King Saud University, Riyadh 11451, Saudi Arabia; msamer@ksu.edu.sa (M.S.A.); mghanem@ksu.edu.sa (M.A.G.); amayouf@ksu.edu.sa (A.M.A.-M.)
2 Department of Chemistry, College of Science, King Saud University, Riyadh 11451, Saudi Arabia; jrajabathar@ksu.edu.sa
3 Division of Photoenergy Conversion Materials, Laboratory for Chemistry and Life Science, Institute of Innovative Research, Tokyo Institute of Technology, R1-26 Suzukake-dai, Midori-ku, Yokohama 226-8503, Japan; nagai.k.ae@m.titech.ac.jp
4 K.A.CARE Energy Research and Innovation, Riyadh 11454, Saudi Arabia
* Correspondence: parunachalam@ksu.edu.sa or prabhuchemist@hotmail.com; Tel.: +966-11-46-96026

Abstract: Visible-light-driven photoelectrochemical (PEC) and photocatalytic water splitting systems featuring heterogeneous semiconductor photocatalysts (oxynitrides, oxysulfides, organophotocatalysts) signify an environmentally friendly and promising approach for the manufacturing of renewable hydrogen fuel. Semiconducting electrode materials as the main constituents in the PEC water splitting system have substantial effects on the device's solar-to-hydrogen (STH) conversion efficiency. Given the complication of the photocatalysis and photoelectrolysis methods, it is indispensable to include the different electrocatalytic materials for advancing visible-light-driven water splitting, considered a difficult challenge. Heterogeneous semiconductor-based materials with narrower bandgaps (2.5 to 1.9 eV), equivalent to the theoretical STH efficiencies ranging from 9.3% to 20.9%, are recognized as new types of photoabsorbents to engage as photoelectrodes for PEC water oxidation and have fascinated much consideration. Herein, we spotlight mainly on heterogenous semiconductor-based photoanode materials for PEC water splitting. Different heterogeneous photocatalysts based materials are emphasized in different groups, such as oxynitrides, oxysulfides, and organic solids. Lastly, the design approach and future developments regarding heterogeneous photocatalysts oxide electrodes for PEC applications and photocatalytic applications are also discussed.

Keywords: photoelectrochemistry; water oxidation; oxynitride; oxysulfide; visible light; organophotocatalyst

Citation: Arunachalam, P.; Nagai, K.; Amer, M.S.; Ghanem, M.A.; Ramalingam, R.J.; Al-Mayouf, A.M. Recent Developments in the Use of Heterogeneous Semiconductor Photocatalyst Based Materials for a Visible-Light-Induced Water-Splitting System—A Brief Review. *Catalysts* **2021**, *11*, 160. https://doi.org/10.3390/catal11020160

Received: 3 December 2020
Accepted: 11 January 2021
Published: 25 January 2021

1. Introduction

The accessibility of an economical, clean, and copious energy source is one of the foremost challenges for humankind in the 21st century. Effective utilization of solar energy and converting it to use fuels that are more appropriate for storage and transportation is mandatory. Solar power provides a clean, renewable energy source with minimal ecological impact since it is a decentralized and virtually unlimited resource. In detail, the solar power reaching the earth's surface is equivalent to that supplied by 130 million power plants of 500 megawatts [1–3]. However, the forthcoming use of solar energy as a major source to satisfy the worldwide requirements depends on accomplishing important milestones of a fundamental and technological nature. The feasibility of the enlargement of solar energy at the terawatt scale depends on finding cost-efficient compatible solutions to these difficulties [4–6].

The manufacture of solar hydrogen (H_2) through PEC water splitting as a proficient and renewable approach to arrest recurrent solar irradiance in the method of chemical fuels has drained remarkable consideration since the revolutionary report by Fujishima and Honda [7]. PEC water photoelectrolysis reaction is determined by solar energy generates an ecological approach to store energy in the covalent bonds of H_2 [8,9]. During earlier stages of research, stoichiometric water splitting was not successful in a theoretical way because of several difficulties, the simultaneous, reverse process, unstable nature of photocatalyst, poor variation in selecting photocatalyst and co-catalyst materials, etc. However, significant advancement has been executed, and many complications and hurdles have been overcome [9–15]. In this context, substantial research efforts have been carried out to upsurge the STH efficiency of those solar-driven photocatalysts. Thermodynamically, the conversion of one molecule of H_2O into H_2 and $\frac{1}{2}$ O_2 is an uphill reaction with a great positive change in free energy change (ΔG° = 238 kJ/mol). In order to efficiently transform solar photons into usable fuels, n-type semiconductor materials can absorb a major portion of the spectral area, with appropriate energy band levels, and lower overpotential to execute a water photoelectrolysis reactions are mandatory. Extensive research efforts have been completed to promote viable n-type semiconducting electrodes that have emerged as photoanodes [14,15].

The oxygen evolution reaction (OER) is mutually kinetically and thermodynamically more exciting, and it hurts from severe oxidizing circumstances [16]. Moreover, the PEC water splitting system is one of the promising methods to examine the electron transfer process in producing oxygen (O_2) in water oxidation reaction to use solar energy [17–21]. In this regard, several oxide-based electrode materials have been investigated [22–35]. On the other hand, all these metal oxides have absorption activity restricted to the UV spectral region due to its wider band gap (>3.0 eV). This is a big drawback since the UV region comprises only 3–5% of all incident solar energy. Further, n-type oxide semiconductor materials such as Fe_2O_3, $BiVO_4$, and WO_3 photoelectrode materials have been extensively applied to gather the visible-light photons for highly proficient as well as steady PEC water splitting system and involve a large external bias [36–45].

It is challenging to develop cost-effective and steady photoelectrodes with STH efficiencies of over 10%. In this regard, a supreme semiconductor light absorber must satisfy a minimum of three simple necessities: (i) its bandgap must be narrow (varied between 1.8 and 2.4 eV) to display a strong light absorption, and its band energy levels must overlap water redox potentials for naturally splitting water into H_2 and O_2; (ii) it must possess great carrier mobilities, and thereby permit quick transport of photoinduced hole-electron pairs from the bulk to the surface; (iv) its surface assembly must be active for water adsorption and successive reactions; (v) it must display lower charge-transfer resistance at the interface. Moreover, highly stable, cost-effective, and ecofriendly photoelectrode materials are mandatory for solar photolysis.

Considering all these conditions for a material to carry out water photolysis (energy levels of the conduction band (CB) and valence band (VB) concerning oxidation and reduction potential of water), most heterogeneous semiconductor-based photocatalysts can also reduce the water. Figure 1 shows the energy for numerous oxide and heterogeneous photocatalysts oxide semiconductors with the water redox reactions, illustrating this fact.

The definite processes in PEC water photolysis are defined in Figure 2. In order to execute this, several steps are needed to gratify the execution of the overall PEC water photolysis reactions. These steps comprise (i) the capture of visible-light photons; (ii) separation of carriers; (iii) transportation of the separated electron/hole pairs through the charge transfer; which need to be catalytically active; and (iv) surface reactions. Both the potential of the excited charge carriers and suitable water oxidation kinetics are mandatory for proficient water photoelectrolysis reactions.

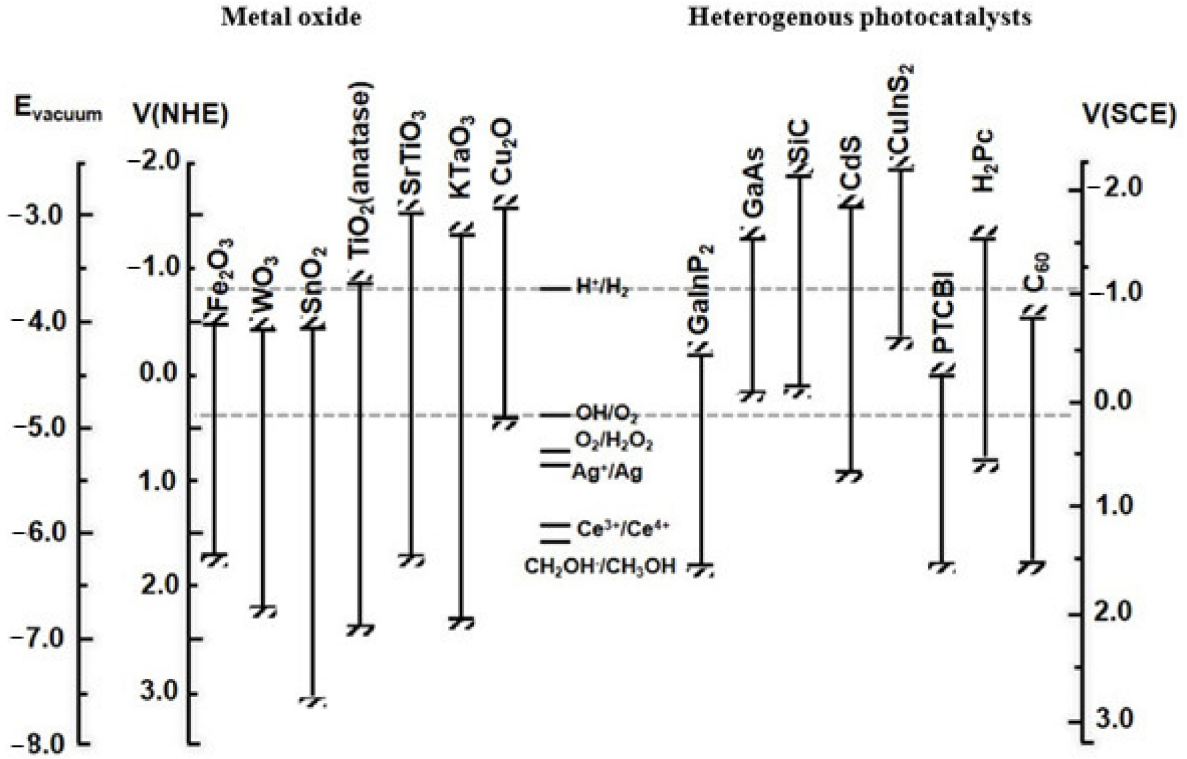

Figure 1. Energy diagram with the conduction and valence band positions for different semiconductor materials. Water oxidation (H_2O/O_2) and reduction potentials (H^+/H_2) are also shown.

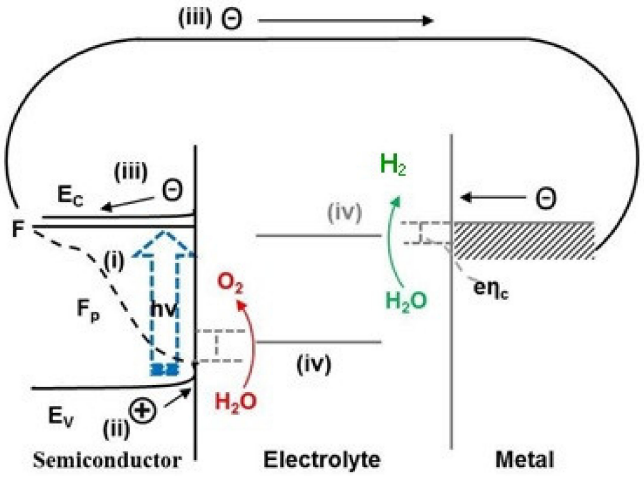

Figure 2. A schematic energy illustration for a photoanodes (n-type semiconductor). Several phases of process are displayed, specifically: (i) light-absorption; (ii) charge-transfer; (iii) transportation of charge-induced electron-hole pairs; and (iv) surface reactions.

In recent years, organic semiconductors (OSCs) with heterojunctions have generally been utilized to construct cost-efficient and effective photocatalysts for photoenergy conversion systems [46–48]. In some cases, photocatalytic reactions via organic p–n bilayers react to the whole visible-light energy for the oxidative elimination of organic pollutants. In another instance, an organic p-n bilayer of phthalocyanine [MPc (M = H_2 or Zn), p-type] and perylene derivatives (3,4,9,10-perylenetetracarboxyl-bisbenzimidazole, PTCBI) or Pt-loaded fullerene (C_{60}, n-type) can act as a photocathode, whereas a reducing power can be produced at the C_{60}/water interface via a sequence of photophysical events in the bilayer [49–52]. Moreover, it was recently evidenced that an organic p-n bilayer can engage near-infrared energy to carry out photocatalysis [53]. In recent years, our group

employed a wet-chemical process of a reprecipitation through a polar solvent in creating biphasic nanocrystals of aluminum phthalocyanine (AlPc)/cobalt phthalocyanine (CoPc) and C_{60} [54–56], whereas earlier reprecipitation developed by Kasai et al. provide a single component of organic crystals whose size, however, is manageable among nanometers to micrometers [57–59].

(Oxy) nitrides are new kinds of materials recently employed as photoelectrode materials for water splitting systems. Oxynitride based photocatalyst tends to possess narrower bandgaps than the equivalent metal oxides since the M-N bond in oxynitrides has potential energy greater than that of the M-O bond in metal oxides. In particular, it must be noted that these kinds of materials vary from photocatalysts doped with N or sulfur [60]. Moreover, (Oxy)nitrides are well-known for their solidity against anodic dissolution in alkaline media, providing them appropriate materials for water splitting applications.[61] Comparatively, certain (Oxy)nitrides photocatalysts can replace metal-oxide-based materials to absorb visible-light photons for water photolysis reactions [61–63]. Similarly, an organic solid/water interface in a p/n organic bilayer was established to be proficient of photoinduced redox reactions combined with photoconduction of the generated hole/electron pairs in the interior [50,64,65], whereas wide-range visible-light energy ($\lambda < 750$ nm) is accessible for the photogenerated redox reactions at the interface mentioned above.

It is projected that long-lasting struggles in this area will result in more fascinating approaches towards emerging durable and high-efficiency heterogeneous photocatalysts based electrodes for water oxidation shortly. This focused review illustrates recent findings in promoting and advancing heterogeneous photocatalyst materials for light-driven water splitting reactions. In this review, heterogeneous photocatalyst materials, such as organophotocatalysts, (Oxy)nitrides, oxysulfides, and other heterogeneous photocatalysts, are presented for solar-driven photocatalytic water splitting, concentrating on recent developments on heterogeneous photocatalyst materials. An outlook for the future growth of heterogeneous photocatalysts-based photoanodes is also projected.

2. (Oxy)nitrides Based Materials

Comparatively, metal nitride/oxynitride based photocatalysts are subjected to photodissociation and have not been employed for water photolysis reaction [66]. In particular, oxynitrides are exceptionally favorable photocatalysts due to their narrower bandgap and subsequent superior visible-light photons related to oxide-based materials. For instance, TaON, Ta_3N_5, and Ba(Ca, Sr)TaO_2N are the distinct classes of (Oxy)nitrides-based families. TaON, whose bandgap is varied from 1.9 to 2.5 eV and energy levels overlap with water redox potentials, is accepted as a more suitable material for developing highly active photoanodes.

The energy level positons of both TaON and Ta_3N_5 are more appropriate for water oxidation and reduction in visible-light conditions. Balaz and co-workers reported the CB and VB's absolute positions of various kinds of characteristic TaON perovskites $ATaO_2N$ (A = Ca, Sr, and Ba) and $PrTaON_2$ [67]. Moreover, TaON and Ta_3N_5 have been widely examined as solar-driven photoelectrode materials in water redox processes [68]. Particularly, above 10% quantum yield has been accomplished with TaON and Ta_3N_5 photocatalysts [69–71]. Domen and co-workers mostly investigated oxynitride based photoelectrodes as an alternative to oxide material, which is likely to arrest the incoming photons for water oxidation reactions [72–74]. In this regard, creating highly active oxynitride-based photoanodes is significant in achieving a high-efficiency PEC water photoelectrolysis process.

Electronic structures of oxynitrides were theoretically investigated in terms of the framework of density functional theory [75,76]. These results illustrate that the N2p orbital has greater potential energy than the O_{2p} orbital; it might be remarkable to engage a metal (Oxy)nitride as a photocatalytic material. In this context, (Oxy)nitrides display distinctive optical features, owing to O_2/N_3 ions' interplay in the system [75,76]. Comparatively, (Oxy)nitrides of the metal system cause a red-shift in the material than oxide-based ma-

terials. This might be owing to incorporating nitrogen (N) into the lattices, whereas the extra energy levels in the host material band considerably affect the optical transition in the system [77]. Particularly, this originated owing to the lesser electronegativity of N to that of O. For instance, Figure 3 compares the schematic representation of the oxide-based $NaTaO_3$ and (Oxy)nitride $BaTaO_2N$, and both of them possess a similar perovskite structure [78].

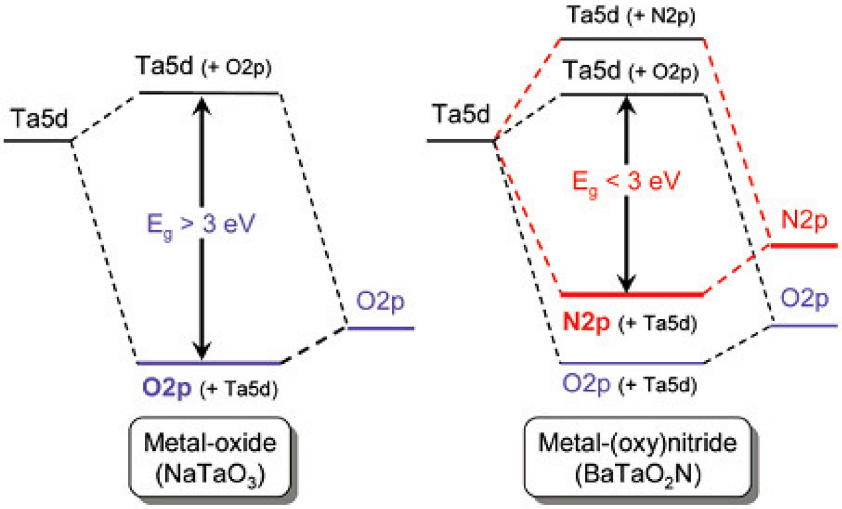

Figure 3. Schematic representation of electronic energy band positions of a metal oxide ($NaTaO_3$) and metal (oxy)nitride ($BaTaO_2N$). Reprinted with permission from Reference K. Maeda and K. Domen, J. Phys. Chem. C, 2007, 111, 7851. Copyright 2007 American Chemical Society [78].

Generally, the most vital parameter affecting photocatalysts' visible-light-driven water oxidation efficiency is the amount of living photoinduced holes directed by the morphology and size of a photocatalyst [79]. In general, the photocatalytic performance can be promoted by means of photoelectrodes with huge surface area, higher dispersion, high crystallinity, reduced defect density, well-defined morphologies, and precisely exposed facets, permitting to decrease the amount of recombination sites and to highly photochemically active sites. In particular, the morphological and structural modification of oxynitrides considerably affects the photocatalytic activity for water oxidation. Also, the flux-assisted nitridation method is beneficial for enhancing the crystallinity, modifying the morphological as well as surface modification of oxynitrides [80,81]. It is also evidenced that the cocatalyst–photoelectrode interface and co-catalysts dispersion over electrodes play a significant part in oxynitride photocatalysis. For instance, Maegli et al. reported the controlled morphological and structural changes of $LaTiO_2N$/CoOx photoelectrodes for photocatalytic O_2 oxidation [82]. They also demonstrated that the flux method improved the crystallinity and higher nitrogen contents in $LaTiO_2N$ than if prepared without flux. In particular, the skeletal and edgy morphology has higher CoOx catalyst dispersion on the $LaTiO_2N$ electrode contained unsaturated bonds, thereby improving the photocatalytic O_2 evolution. Moreover, Kodera et al. demonstrated that flux treatment on $BaNbO_2N$ photoelectrodes greatly influenced the morphological natures [83]. Prior to flux action, the $BaNbO_2N$ morphological features were uncertain, with an accumulation of particle sizes varied from a few 10′ s nm to 100′ s nm. After the flux treatment, a noticeable modification in morphology happened. Figure 4 displays FE-SEM images of $BaNbO_2N$ photocatalysts before and after flux action. After flux treatment, a cubic morphology was clearly noticed. Similar flux-influenced morphological modifications are also demonstrated for $BaTaO_2N$ crystal structures [84]. Thus, the flux-aided nitridation process is mandatory to promote oxynitride's photocatalytic features by enhancing crystallinity, tailoring the morphology and surface modifications, reducing the defect density.

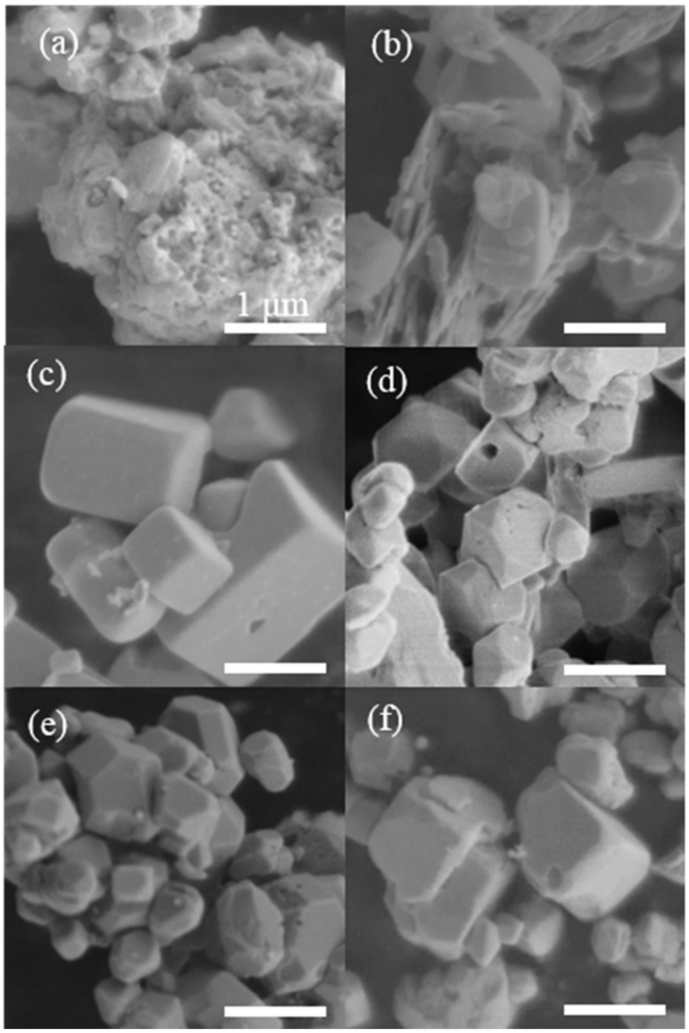

Figure 4. FE-SEM photographs of obtained $BaNbO_2N$ particles (**a**) before and after flux treatment with (**b**) LiCl, (**c**) NaCl, (**d**) KCl, (**e**) RbCl, and (**f**) CsCl. Scale bars represent 1 μm [83].

Different (Oxy)nitrides materials have been considered to replace the oxide catalysts to capture the light-photons to produce H_2 and O_2 from water at the stoichiometric ratio [85–90]. Afterwards, these kinds of (Oxy)nitride-based photoelectron materials are well-known for PEC water oxidation, with nominal input [91,92]. A large quantity of such (Oxy)nitride photoanodes have been reported to date. Moreover, few of them attained superior incident photon-to-current efficiency (IPCE) efficiency of >10% with an applied bias lesser than the thermodynamically needed bias (1.23 V) for water photoelectrolysis. Further, in the case of wavelength, light photons with wavelengths up to 600 nm are accessible for PEC water oxidation with Ta3N5 [93] and $LaTiO_2N$ [94]. In this regard, no narrower photoanodes (<2.0 eV~equivalent to 600 nm) are available to oxidize water without any externally applied bias has been demonstrated till now. Furthermore, while decreasing the photoanodes' bandgap, reducing the driving powers for water redox reactions makes water electrolysis reactions more challenging.

Both the superior performances and stability of (oxy)nitrides for PEC water electrolysis rely on the effective transfer of the photoinduced holes from the photoelectrodes to reactants adsorbed on the surface to induce the water oxidation for OER. Building a catalytic active surface morphology for PEC water electrolysis is extremely required to advance surface charge transfer. In particular, the catalytic surface must provide the roles of gathering photoinduced holes, permitting ample adsorption of water molecules and making it a lower reaction kinetic barrier for the oxidation reaction. Despite its abil-

ity to capture solar energy and chemical inertness, the PEC behavior of (oxy)nitrides is bizarrely restricted due to its deprived photon absorption, the greater recombination rate of photogenerated carriers sluggish OER kinetics. To rectify these drawbacks, (oxy)nitrides photoanodes must be loaded with co-catalyst materials to promote light photon absorption. During the last decades, numerous works have been carried out to advance (oxy) nitride-based photoanodes with appropriate co-catalysts to efficiently utilize visible light photons [63,92]. Moreover, much attention has been paid to develop (oxy)nitride-based photoanodes loaded with cost-effective transition metal oxides. Nishimura al. demonstrated the TaON based (oxy)nitrides along with co-catalyst photoanodes and attained IPCE of 76% at 400 nm with a nominal external bias [92]. Subsequently, different (oxy)nitrides, such as $LaTaO_2N$ [94], $SrNbO_2N$ [95–97], and $BaNbO_2N$ [98], among others, have been newly advanced as photoanodes [99–103].

Photoelectrodes with catalytic surface modification of several co-catalysts for water electrolysis, namely IrO_2, CoOx and "Co-Pi" have been deeply examined [102–109]. In particular, Abe and co-workers reported incorporating $IrO_2.nH_2O$ nanoparticles over porous TaON photoanodes and have achieved the IPCE of 76% in an aq.Na_2SO_4 solution [109]. Further, it is the first report to demonstrate the PEC water splitting on TaON (oxy)nitride with a scannable production of O_2, as well as measured anodic photocurrent. Notably, Higashi et al. reported a methodology of pre-depositing earth plentiful CoO_x co-catalysts over TaON particles via impregnation before the electrophoretic deposition (EPD) of TaON particles [106]. Recent years, (Oxy)nitrides photoelectrode materials, namely $LaTiO_2N$/CoOx, $BaTaO_2N$/$BaZrO_3$, and $BaNbO_2N$ [110–113], have been developed to exploit the visible-light photons absorption with the supporting sacrificial reagents. Much research has mainly focused on creating the visible-light active narrower bandgap semiconductors photoanodes (<2 eV). In this regard, Zhang et al. reported $LaTaO_2N$ photocatalysts materials prepared through the flux technique. It also revealed enriched PEC behavior for the water oxidation reaction [114]. Quite recently, new kinds of rare earth hafnium ($RHfO_2N$) (Oxy)nitride were demonstrated for the photocatalytic water redox reactions [77,115]. The $RHfO_2N$ perovskites (R = La, Nd and Sm) signified the $GdFeO_3$-type structure with a bandgap energy of 3.35, 3.40, and 2.85 eV. These hafnium-based materials photocatalytic results revealed $RHfO_2N$ oxynitrides that have been successfully applied towards overall water splitting reactions. Also, Takata et al. have demonstrated and activated $LaMg_xTa_{1-x}O_{1+3x}N_{2-3x}$ photocatalysts for photocatalytic water splitting by incorporating the co-catalyst of RhCrOx [116].

Niobium-based oxynitrides are of specific interest in water splitting owing to their narrow bandgap of 1.7 eV, while it was evidenced to be satisfactory for photocatalytic water photodissociation [117]. Maeda et al. first reported the narrower bandgap semiconductor of FTO/$SrNbO_2N$ photoanodes (<2.0 eV) substrate via electrophoretic deposition (EPD) process and examined for water splitting reactions under neutral conditions.[118] IrO_2 incorporated $SrNbO_2N$/FTO electrodes chronoamperometric (CA) investigation showed significantly improved PEC water oxidation behavior compared to $SrNbO_2N$/FTO as presented in Figure 5A. During the CA analysis, an external bias of 1.55 V_{RHE} was engaged under steady-state light irradiance ($\lambda > 420$ nm). The enhanced performance was accredited to the substantial role of adsorbed IrO_2 colloids over $SrNbO_2N$ particles to suppress the material's oxidative self-decomposition and thereby enhance the selectivity of photoinduced holes toward water oxidation. This is an efficient approach to improving the PEC performances in the lower potential region, thereby promoting water oxidation. The authors further evidenced the water oxidation by evaluating the stoichiometric generation of H_2 and O_2 upon irradiation and was shown in Figure 5B. Moreover, in terms of evolved H_2 and O_2, the authors estimated that 47% of the visible-light current might be credited to photogenerated water oxidation by IrO_2/$SrNbO_2N$.

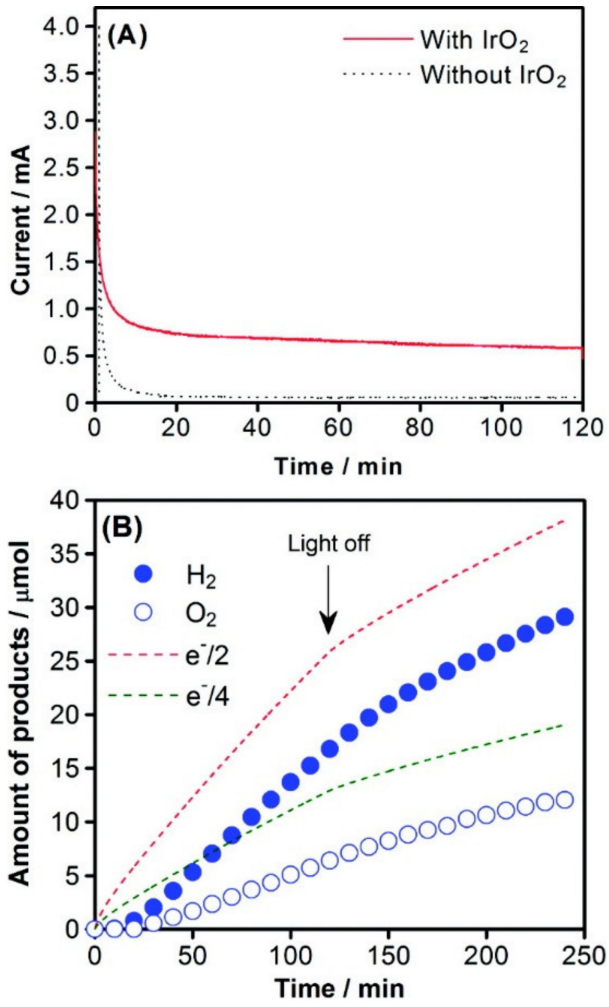

Figure 5. (**A**) Photocurrent-time plots in aq. 0.5 M Na_2SO_4 (pH ≈ 6) for $SrNbO_2N$ photoelectrodes (6 cm^2) with and without colloidal IrO_2 at +1.55 V_{RHE} under visible-light conditions (λ > 420 nm). (**B**) and its equivalent time progresses of gas evolution in PEC reactions by an IrO_2-loaded electrode. Reprinted with permission from Reference K. Maeda, M. Higashi et al. J. Am. Chem. Soc., 2011, 133, 12334. Copyright 2018 American Chemical Society [118].

In recent years, we also demonstrated the PEC activity of cobalt phosphate (CoPi)/ La(Ta,Nb)O_2N and CoPi/$ZnTaO_2$N electrodes for PEC water oxidation in alkaline conditions [99,119], which showed up to a nearly four-fold advancement in the PEC activities at a lower oxidation potential. In particular, the loading of the CoPi over (Oxy)nitride photoanodes might promote the charge separation as well as the carrier collection created at the electrode surface, thereby improving PEC features of the photoanodes). We have also recently reported the CoPi loaded $ZnLaTaON_2$ photoanodes for PEC water oxidation performances under alkaline solution [120]. In all these cases, the photodeposition (PD) of CoPi onto (oxy)nitrides photoanodes under irradiation conditions were evidenced to promote the OER at the photocatalysts [121]. Further, the CoPi co-catalyst layer was incorporated over (oxy)nitrides by employing the in-situ PD approach to promote the OER half-reaction kinetics. We have also evidence that the CoPi deposition's magnitude was determined by the electrodes' morphology, time, and loading process method. The thicker CoPi incorporation over (Oxy)nitrides photoanodes resulted in the poorer PEC behavior for water oxidation. These facts can be illustrated that the photocatalytic water oxidation reaction happens at the CoPi/electrolyte interface. In the thicker CoPi, the photoinduced holes need to transfer between more number CoPi molecules and a CoPi/electrolyte interface. Subsequently, a decline in photocurrent is witnessed. However, in thin CoPi

layer over (oxy)nitrides, associated cobalt ions on (Oxy)nitrides surface easily capture the photoinduced holes to yield the active catalytic species of cobalt (Co^{4+}) mandatory for a water electrolysis reaction [122,123]. Likewise, amorphous $Co(OH)_x$ has been used as a co-catalytic material for water oxidation reaction and can enhance the PEC stability as well as performances of Ta_3N_5 photoanodes [122–125], even though it is not as efficient as CoPi. One of the major roles for superior performance of CoPi co-catalyst in comparison with $Co(OH)_x$ is the whole coverage of Co-Pi on the Ta_3N_5 photoanodes. Generally, in $Co(OH)_x$ is incorporated over Ta_3N_5 photoanodes surface via the co-precipitation process; thereby, it is hard to obtain the homogeneous dispersion by PD method. Thus, the PD methodologies benefit from permitting the comparatively homogeneous wrapping of CoPi over the (Oxy)nitride surface of the photoanodes. These results show that the incorporation of CoPi over (Oxy)nitride has been an efficient route to enhance the PEC current gain via the PEC water oxidation reaction.

Like CoPi electrocatalysts, layered double hydroxides (LDHs) have been widely investigated as catalytic materials for water oxidation [126,127]. Particularly, LDHs attained by a solution exfoliation process revealed greater OER performances and improved durability compared to noble metal/metal oxide electrocatalysts. Mostly, LDHs co-catalysts were engaged to promote the PEC performances for water electrolysis reaction [128]. In this regard, Wang et al. reported the Ni–Fe LDHs incorporated Ta_3N_5 photoanodes array and are significantly enhanced stability and PEC performances for water oxidation [129]. Further, the author's group deposited the Co(OH)x and CoPi electrocatalysts on sequence over Ni–Fe LDH/Ta_3N_5 photoanodes, further enriched the photocurrent. Liao et al. associated the effect of various co-catalysts ($Co(OH)_x$, Co_3O_4 and IrO_2) and electrolytes (NaOH and Na_2SO_4) on the photocurrent and superior durability of photoanodes comprising of nanoparticulate Ta_3N_5 [130].

Allam and co-workers recently reported a novel photoanode material of Ti-Pd mixed (Oxy)nitride films prepared through anodization method and attained a photocurrent density of 1.9 mA/cm^2 and a nearly five-fold enhancement in the efficiency compared to pure TiO_2 nanotubes [131]. Similarly, titanium oxynitride (TiON) emerges as a favourable candidate for light absorption and appropriate energy level positions for water splitting [132,133]. In particular, Soliman et al. fabricated the TiON nanotube arrays via NH_3 nitridation from anodized Ti foil. Very recently, Soliman et al. demonstrated the highly ordered Ag nanoparticles incorporated TiON nanotubes arrays for solar-driven water splitting [134]. Further, the author group investigated PEC properties of Ag/TiON nanotubes arrays resulting in an exceptionally superior photocurrent of 14 mA/cm^2 at 1.0 V SCE (Figure 6b), which is consistent with the absorption spectra (Figure 6a). The observed improvement of photocurrent over TiON counterparts is credited to co-operative features of Ag nanoparticles incorporation, N-doping, and the distinctive morphological characteristics of the fabricated NTs arrays. In detail, the IPCE measurements of Ag/TiON nanotube arrays with the potential between 0.2 V and 0.4 V (Figure 6d) evidences the maximum IPCE of 41% in the wavelength ranging between 450 and 510 nm and is comparatively superior to TiON nanotubes arrays (Figure 6c).

Table 1 summarizes studies on different (Oxy)nitride-based electrode materials for solar light-driven water splitting reactions. The electrodes presented in Table 1 and the co-catalysts' deposition significantly improved the PER performance with higher durability for solar-water splitting. In recent years, (Oxy)nitrides-based electrode materials have gained much consideration. They must be investigated in numerous ways, namely morphological features, co-doping strategies, defect induced features, surface activation, co-catalyst loading, etc. These examinations on the (Oxy)nitride photoelectrode materials basically lead to a more detailed understanding of their effective usage in the water-splitting system.

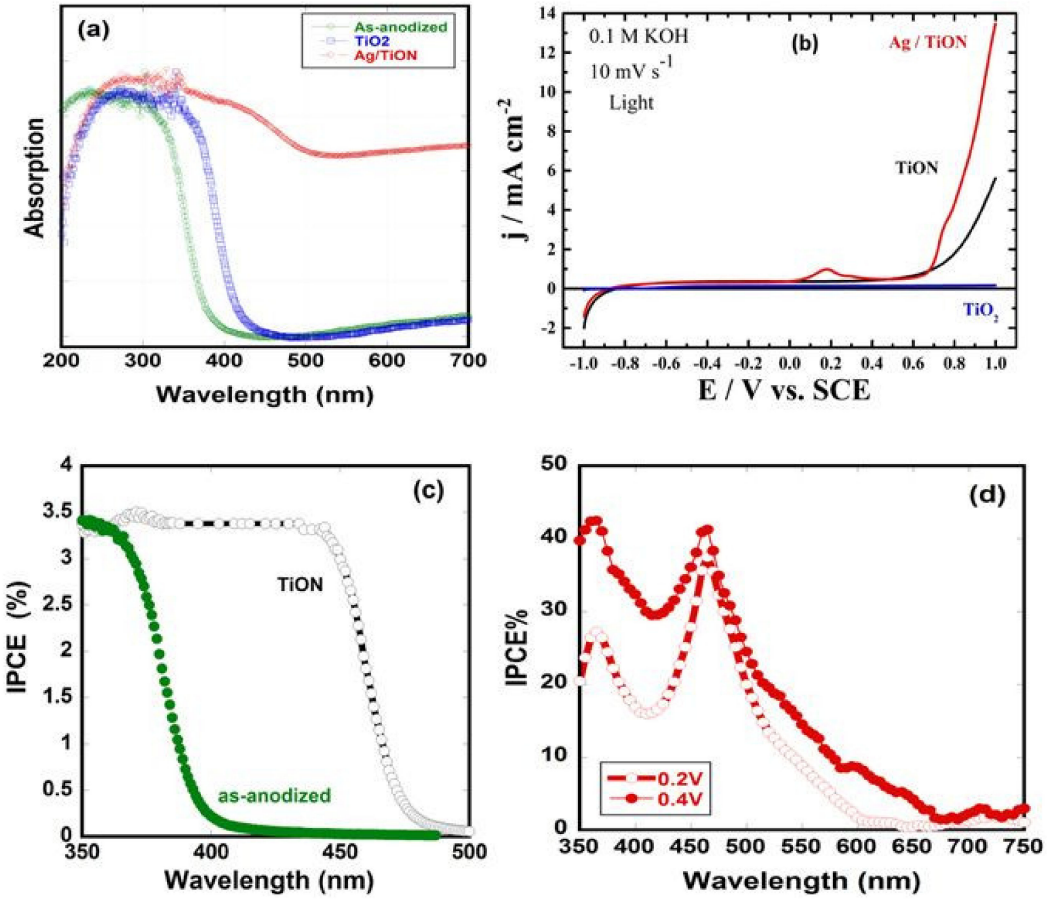

Figure 6. (**a**) UV-Vis absorption analysis of NTs, air annealed TiO_2 NTs, and Ag incorporated TiON NTs (Ag/TiON), (**b**) LSV plots under the irradiation of TiO_2, TiON and Ag/TiON, (**c**) the IPCE spectra of the samples, and (**d**) the IPCE of Ag/TiON electrodes under externally applied bias [134].

Table 1. Review on different kinds of (Oxy)nitrides based photoelectrodes with co-catalysts and their photoelectrochemical features for water splitting reactions.

Electrodes	Cocatalysts	Synthesis Method	Photocurrent(j)	Efficiency IPCE (@1.23 V vs. RHE)	Stability	Reference
$LaTiO_xN_y$	IrO_2	magnetron sputtering	70 μA cm^{-2} at +1.0 V vs. Ag/AgCl	-	30 min	[90]
$LaTiO_2N$	In_2O_3	Electrophoretic deposition (EPD)	0.61 mA cm^{-2} at 1.23 V_{RHE},	3.2% at 400 nm	30 min	[135]
$SrNbO_2N$	IrO_2	Polymer Complex(PC)/EPD	0.35 mA cm^{-2} at +1.2 V vs. RHE	0.2%	2h	[118]
TaON	$CoOx/TiO_2$	screen-printing	0.7 mA cm^{-2} at +1.2 V vs. RHE	27% at with λ = 410 nm	15 h	[136]
$BaTaO_2N$	CoO_x/RhO_x	EPD	-	10% at 600 nm	60 min	[137]
$BaNbO_2N$	$FeO_x/Co(OH)_x$	particle transfer (PT)	5.2 mA cm^{-2} at 1.23 V_{RHE},	38% at with 460 nm	« 30 min	[138]

Table 1. *Cont.*

Electrodes	Cocatalysts	Synthesis Method	Photocurrent(j)	Efficiency IPCE (@1.23 V vs. RHE)	Stability	Reference
$SrNbO_2N$	CoO_x	magnetron sputtering	4.1 mA cm^{-2} at +1.2 V vs. RHE	10% λ = 400 nm	–	[139]
$BaTaO_2N$	Co	PT	4.2 mA cm^{-2} at 1.2 V_{RHE}	24% with λ = 400 nm	6 h	[140]
$SrNbO_2N$	CoPi	flux treatment/PT method	1.5 mA cm^{-2} at 1.23 V_{RHE}	-	2 h	[141]
$BaNbO_2N$	-	Flux treatment/PT	5 mA cm^{-2} at 1.23 V_{RHE}	-	-	[142]
$CaNbO_2N$	Co-Pi/Al_2O_3	solid state/PC	70 μA cm^{-2} at 1.23 V_{RHE}	-	30 min	[109]
$CaTaO_2N$-A	NiB	EPD	40 μA cm^{-2} at 1.23 V versus RHE	-	-	[143]
$SrNbO_2N$-NRs	-	PT	1.3 mA cm^{-2} at 1.23 V_{RHE},	-	15 min	[144]
$SrNbO_2N$	Co_3O_4	EPD	2.0 mA cm^{-2} at 1.23 V_{RHE}	12% with 420 nm	30 min	[145]

3. Oxysulfide Based Photocatalyst

Oxysulfides are new kinds of fascinating photocatalytic materials in heterogeneous based semiconductors photocatalysts. Similar to (Oxy)nitrides, the main idea of combining sulfur into oxides is basically the same as that for N incorporation. Particularly, the oxysulfides recognized as stable photocatalyst form than its corresponding metal oxides. Its energy level positions are appropriate for water photoelectrolysis reactions. In particular, oxysulfides comprise S as a constituent element that forms the tops of the VB. Thus, the sulfur loading usually reduces the bandgap compared to its counterparts of the corresponding oxide by developing shallower filled energy states than O 2p states. Thereby, photoinduced holes can travel smoothly in the VB of the material, predominantly beneficial for water oxidation concerning the 4-electron transfer. Till now, overall water splitting through an independent oxysulfide is yet to be developed. In contrast, few oxysulfides based photocatalysts are applied to PEC water electrolysis reaction with bias assistance, tandem style, or Z-scheme, water splitting.

Ishikawa et al. reported the stable oxysulfide of $Sm_2Ti_2S_2O_5$ with a wide absorption band in the visible-light region (λ < 600 nm) and band edge potential are more appropriate for overall water splitting [146]. These oxysulfide photocatalysts can be attained by annealing the mixture of equivalent precursors under vacuum and subsequently processed for sulfurization through H_2S gas [147]. Density function theory calculations further evidence that the S_{3p} atomic orbitals constitute the upper region of the VB of $Sm_2Ti_2S_2O_5$ and provide a significant influence in lowering the bandgap energy to its counterpart of metal oxide ($Sm_2Ti_2O_7$). Further, metal sulfides such as CdS are not appropriate to engage as a catalytic material for water oxidation due to the integral unstable nature of these electrode materials in the reaction through the photoinduced generation of holes [148,149]. In contrast, $Sm_2Ti_2S_2O_5$ performed as a relatively stable photoelectrode material for water electrolysis reaction. Similar to (Oxy)nitride, the photooxidation performance of the oxysulfides will be improved by incorporating the colloidal IrO_2 over $Sm_2Ti_2S_2O_5$, thereby increasing the quantum efficiency for O_2 generation to 1.1% [150,151]. Moreover, physical characterization evidence that the decomposition of oxysulfide in bulk and at the surface,

in precise the oxidation of S^{2-} species, does not happen throughout the photooxidation of water. Quite recently, Ma et al. reported the $Sm_2Ti_2S_2O_5$ via novel flux method and demonstrated its photocatalytic activity is promoted by incorporating IrO_2 co-catalyst and Pt over oxysulfides. Further, Z-scheme visible-light assisted water splitting into H_2, and O_2 was evidenced by applying the oxysulfides photocatalyst for H_2 production combined with an H-CS-WO_3 photocatalyst (shown in Figure 7) [152]. These results conclude that the oxysulfide $Sm_2Ti_2S_2O_5$ behaves as a highly stable photoelectrode material for water redox reactions under visible-light illumination. Similarly, other kinds of $Ln_2Ti_2S_2O_5$ (Ln: Pr, Nd, Gd, Tb, Dy, Ho, and Er) oxysulfides with similar layered perovskite structure are recognized as active and stable electrode materials for water photoelectrolysis reactions with supporting electrolyte comprising a sacrificial electron donor or acceptor [153]. Likewise, Zhang et al. developed that $Ln_2Ti_2S_2O_5$ compounds (absorption edge at ca. 600 nm) evidenced photocatalytic behavior for water electrolysis reaction with appropriate support sacrificial reagents [154]. Moreover, this is the first $Ln_2Ti_2S_2O_5$ oxysulfide to behave as a photocatalyst for the water oxidation reaction. Similarly, Ogisu and co-workers developed the visible-light responsive $La_5In_3S_9O_3$ and $La_3GaS_5O_{14}$ oxysulfide photocatalysts and investigated water electrolysis reaction with a proper hole or electron scavenger(s) under irradiation conditions [155–157].

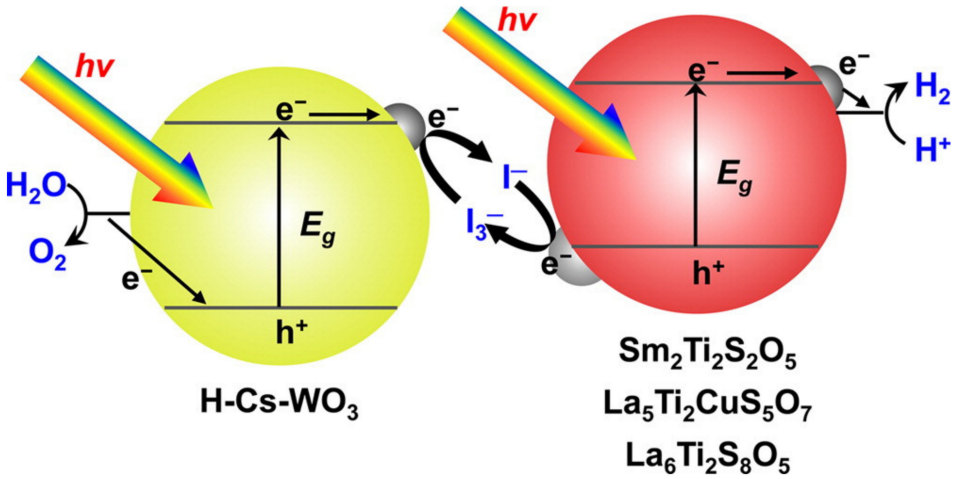

Figure 7. Schematic representation of the oxysulfide system employed for visible-light-driven Z-scheme water splitting into H_2 evolution in conjunction with Cs loaded WO_3 photocatalysts. Reprinted with permission from Reference G. Ma, S. Chen et al. J. Phys. Chem. Lett, 2016, 7, 3892. Copyright 2016 American Chemical Society [154].

These oxysulfides based electrodes reveal remarkable PEC behaviors. Usually, p-type semiconductors behave as photocathodes, and generate H_2 at the boundary between the semiconductor and the electrolyte. In particular, most of the sulfides are naturally an n-type semiconductor, while Cu^+ -containing sulfides tend to behave as p-type semiconductors. In this regard, Liu et al. reported the Cu^+-containing oxysulfide $La_5Ti_2CuS_5O_7$ photocathode via the particle transfer method. In contrast, doped oxysulfides show an 8-fold enhancement compared to their counterparts for PEC water splitting reaction [157]. Likewise, Ma et al. reported the $La_5Ti_2CuS_5O_7$ oxysulfides enabling to act both as photocathodes and photoanodes by tuning its work functions and employing them as electrodes in the water-splitting reaction [158]. Similarly, Hisatomi et al. reported the new kinds of oxysulfides $La_5Ti_2Cu_{1-x}Ag_xS_5O_7$ photocathodes, functioning at the operative potential for PEC H_2 evolution under solar-light irradiance [159].

4. Other Heterogeneous Photocatalysts

As an alternative to oxides, Yoshimizu attempted new kinds of silicide based photocatalyst (Iron disilicide β-$FeSi_2$) composed of abundant, durable, and non-toxic elements [160]. In particular, the author investigated the β-$FeSi_2$ catalyst material for H_2 evolution cata-

lysts because it possesses appropriate conduction band energy levels and succeeded an obvious quantum efficiency of 24% upto 950 nm support of a sacrificial agent. Similarly, Akiyama et al. succeeded in fabricating the semiconducting β-$FeSi_2$/Si composite through the vapor-liquid-solid method. They investigated the photocatalytic H_2 behavior with the support of the formaldehyde as a sacrificial agent [161]. As an H_2 evolution photocatalyst, β-$FeSi_2$ is projected to be sensitive to near-infrared light (>1300 nm), which is the longest wavelength of light to be used. Recently, Akiyama et al. fabricated the β-$FeSi_2$/SiC composite powder and evolved H_2 under the visible light photons with methyl alcohol as a sacrificial reagent [162].

Similar to heterogeneous photocatalysts, metal-free photocatalysts are favorable photocatalytic materials that have not been widely investigated. On this phenomenon, Wang et al. demonstrated a new class of metal-free graphitic C_3N_4 (g-C_3N_4) based material and employed as photocatalysts for water splitting reactions under visible-light photons [163,164]. In this regard, few kinds of metal-free photocatalytic materials are presently available: g-C_3N_4, $C_3N_3S_3$ [165], a-sulfur [166], red phosphorus [167], black phosphorus [168], and organic ones as below. However, all these metal-free photocatalysts require scarce/expensive noble metal co-catalysts to be active for PEC water splitting reactions [169]. Fortunately, boron carbide and hexagonal boron carbon nitride (h-BCN) are fascinating new kinds of proficient metal-free and light-active photocatalysts for water splitting reaction. Liu et al. developed the boron carbides as photocatalytic materials for H_2 production. They achieved H_2 production of 14.5 μmol h^{-1} g^{-1} without any co-catalysts [170].

5. Organic Photocatalyst (Organophotocatalyst)

Generally, organic materials have run after inorganic ones that exhibit high electromagnetic properties due to high electron density and various elements such as conductions, magnetism, optics, etc. Organophotocatalysis based system exhibits an innovative technique for water splitting reactions exploiting energy over the whole range of visible light.

Primary reports designated photocathodes made from conducting polymers, namely polyacetylene [171–173], polypyrrole [174], polyaniline [175,176], poly(3-methylthiophene) [177] or poly(3-hexylthiophene), P3HT [178,179], phthalocyanine [180–184]. Organic photocatalyst without electrode also has a long history using poly(*p*-phenylene) [185–187] etc. Conversely, these photocatalytic materials did not comprise any junction between OSCs and charge separation from the Schottky junction between p-type OSC and electrolyte and kinetically low efficiency.

The closest research field of organic photovoltaic (OPV) devices to organic photocatalyst becomes more than 14% power conversion efficiency from the sunlight [188], and organic photocatalysts would have promising high efficiency in the near future if the stability problem is solved. Besides general merits in organic materials such as fabrication process varieties, flexibility, low density, and solubility, there are great merits of huge variety to control electronic properties in light absorption with a pi-system, conducting polymers nanostructures, e.g., synthetic metals or phase separations of bulk heterojunction [189–195]. As shown, the first p-n junction OPV [196] exhibited unidirectional electron-hole transfer path at both interfaces and the potential difference is derived by the photo illumination as visible-light-induced charge creation is succeeded at the boundary between the two OSCs as shown in Figure 8. Upon absorption of visible-light photons in one of the OSCs, an exciton is created and then transported to the junction with another OSC. At this point, the exciton dissociates, resultant in the arrival of a hole in one OSC called the donor, and an electron in the other OSC called the acceptor. In photovoltaic systems, charge carriers then transport to the electrodes where charges have been collected. These concepts are useful to design an efficient PEC system. By choosing a bilayer system, photoinduced charge separation becomes efficient in the case of PEC also [52]. Furthermore, various modifications gave more efficiency, such as p-n interface [197] and liquid/electrolyte interface [198]. Low cost and water-based synthesis of p-n junction like nanoparticles are possible to mass productively [46–48]. By combining polymer substrate, macroscopic separation of

redox site is possible [49], and multilayerization of the photocatalyst film [47] exhibit more efficient utilization of natural light. The utilization of longer wavelength reaching to near-infrared is also attractive to utilize the sunlight [48,199]. Very recently, lateral charge separation to the substrate direction was discovered for step shape electrode using Kelvin probe force microscopy [200]. It is noteworthy that phthalocyanine has another role as a catalyst. One of the evidential phenomena is P3HT/PCBM photoanode [201,202], where coating with co-catalyst phthalocyanine enhanced photoanodic current. A recent observation by Kelvin force probe microscopy reveals a dipole formation between the co-catalyst and bulk heterojunction (BHJ), suggesting efficient charge separation for multi-electron transfer [202].

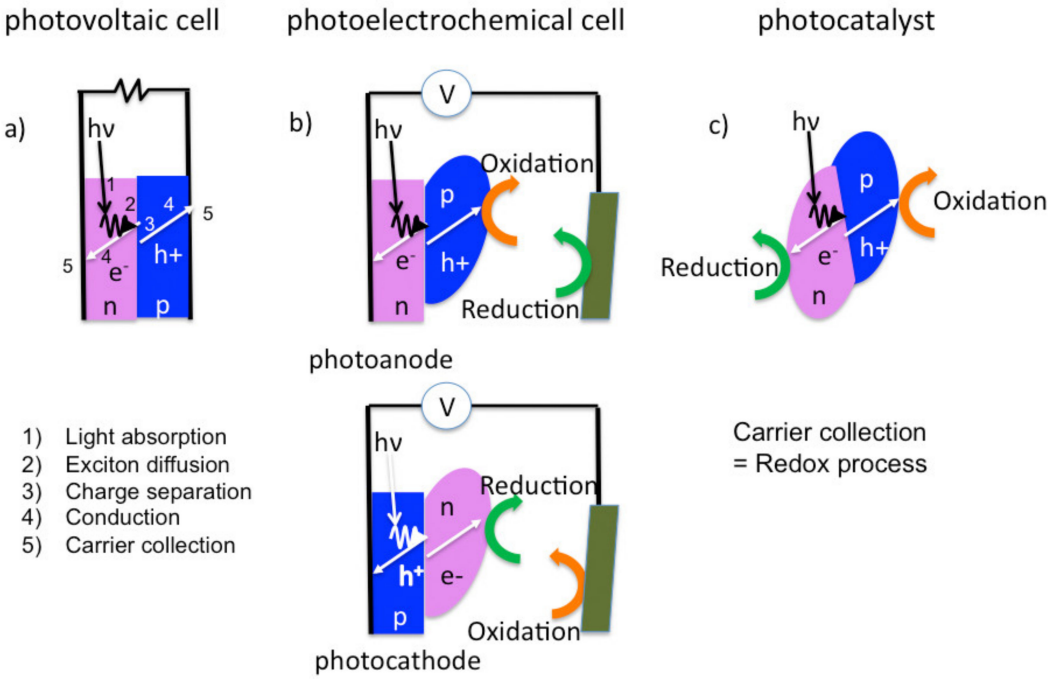

Figure 8. Schematic view of p-n junction photovoltaic cell (**a**), PEC (**b**), and photocatalyst (**c**). There are five common processes, while the final methods of carrier collections are different. Reprinted with permission from *Kobunshi Ronbunshu.*, vol. 70, page 461. Copyright 2013, The Society of Polymer Science, Japan [202].

The main concern is the arrangement of the two different things since excitons can only diffuse in the range of few tens of nm for the duration of their lifetime, i.e., beforehand spontaneous recombination happened. As a result, the two OSCs must be either loaded as two very thin layers, probably with an interlayer comprising both constituents, resulting in a mixture of the two materials creating molecular p-n junctions all over the bulk layer BHJ. More importantly, BHJ is made between a polymer or an array of small molecules, performing as the light absorber, and a C_{60} derivative [195] typically. In order to employ such organic junctions in direct PEC water splitting, there are similarities in the continuous processes as above, while dissimilar conditions must be seen at the interface between the organic layer with a liquid electrolyte.

OER has a more crucial issue that strongly relates to stability and efficiency problems due to multielectron oxidation and co-existing thermodynamically easy path of photoanode etching. However, OER in an aqueous medium was validated with organic polymer catalysts/electrolyte solution junctions, obtaining photocurrent densities in the range of a few microamperes [203–205], or more bias potential [206]. Saline oxidation is one of the smart systems as alternative oxidation of chloride ions [207,208]. Coating of the metal oxide layer is another choice for long term stability [209–214].

Pt nanoparticles are good HER catalyst and were incorporated over the uppermost of an organic p/*n* bilayer electrode of small moieties (metal-free phthalocyanine, H_2Pc/C_{60}),

photocurrent values grasped several cents of $\mu A.cm^{-2}$ and the faradic efficiency for H_2 evolution in aqueous media reached nearly 90% (Figure 9) [45]. H_2 generation at Pt-attached C_{60}/water interface utilizes electrons from the CB of the C_{60} layer. While the lowest of the CB of C_{60} is less negative than H_2 evolution, the production of 2-electron reduced C_{60}^{2-} species was demonstrated spectroscopically after a 20-min induction period.

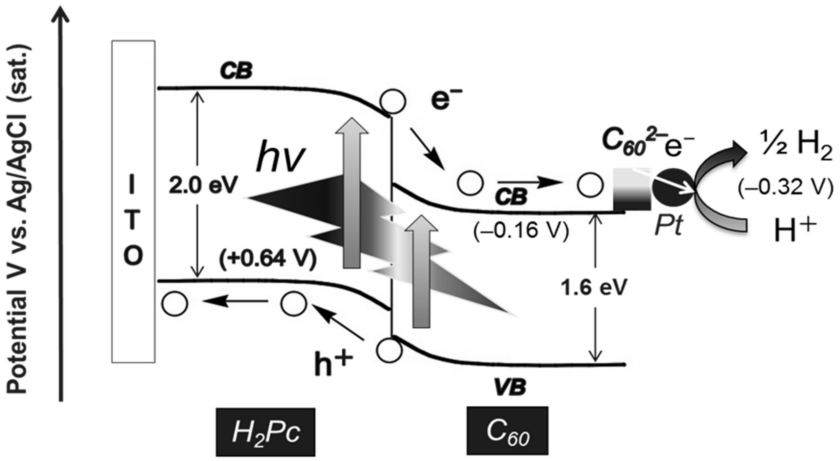

Figure 9. Schematic representation of visible-light-assisted H_2 generation in the organic ITO/H_2Pc/C_{60}-Pt system. H_2 evolves at Pt-loaded C_{60}, after a 20 min period during which C_{60}^{2-} is formed. Reprinted with permission from *The Journal of Physical Chemistry C.*, vol. 115, page 7704. Copyright 2011, American Chemical Society [45].

The organic electrode presented in Figure 10 comprises photoelectrodes based on OSC to oxidize thiol [215], based on TiO_2 to oxidize water [216], hydrazine oxidation [217] or borane-ammonia [218]. By employing photoelectrodes, H_2 can be produced without additional electric bias. In this case, concomitant H_2 evolution takes place at the Pt electrode without any input. Our research group recently investigated the photocatalysis system comprising an organic p/n bilayer for the stoichiometric degradation of hydrazine into N_2 and H_2 [218]. In this regard, these works illustrate the H_2 generation by reducing power photoinduced at the PTCBI in an organic p/n bilayer.

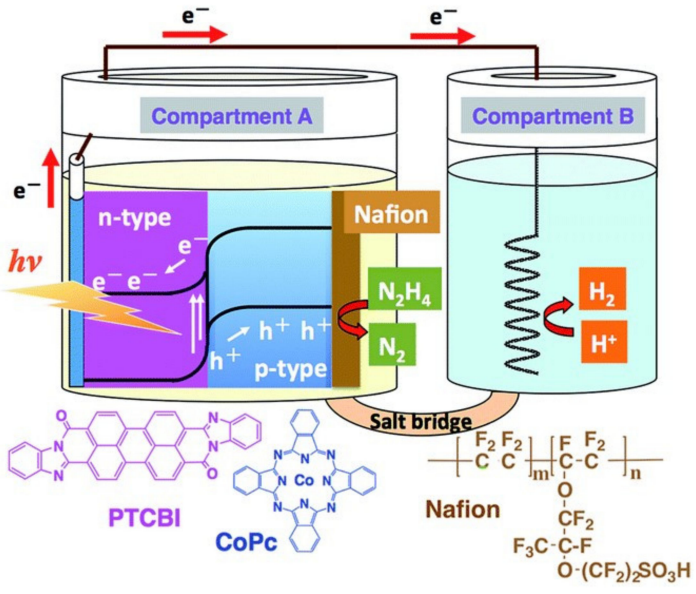

Figure 10. Twin-compartment cell utilized for one active electrode photocatalysis and the structures of the chemicals. Reproduced from Ref. [219] with permission from the Royal Society of Chemistry [219].

Our research group recently reported the PEC system containing an organic-based photocathode of a p/n bilayer (ITO/ZnPc/C_{60}–Pt) alongside a WO_3 photoanode, where a stoichiometric generation of H_2 and O_2 was initiate to happen (Figure 11) [220]. In this system, oxidation and reduction powers can be markedly produced at the tungsten oxide photoanode and organo-photocathode, correspondingly. In this context, electron transport from tungsten oxide CB to the hole continued p-type VB in the organic p/n bilayer can proficiently happen for executing the PEC method, accordingly effecting a high concentration of carriers, which is readily existent for rate-limiting O_2 evolution at photoanodes for effective charge separation. Finally, combining the two different water splitting materials is an efficient approach to developing a Z-scheme photocatalytic system.

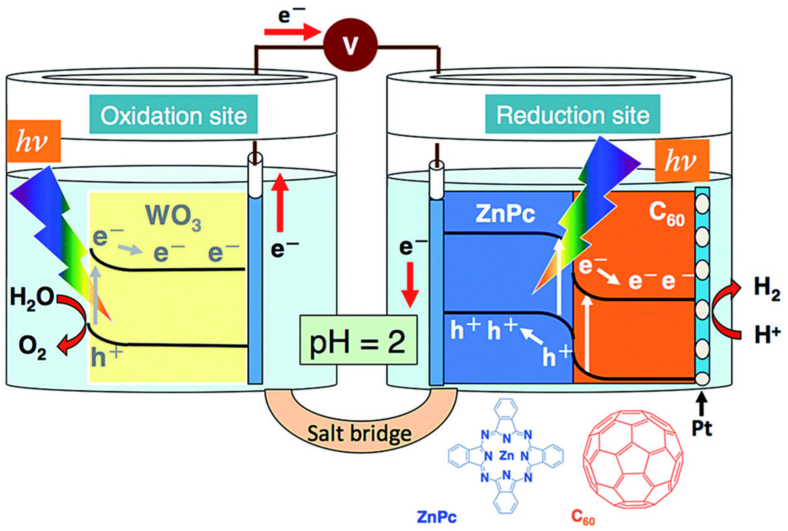

Figure 11. A schematic representation of the water-splitting system comprising an organo-photocathode and WO_3 photoanodes. Reproduced from Ref. [220] with permission from the Royal Society of Chemistry [220].

The recent trend to use OSM is to be covered with a thin inorganic layer, for example, amorphous molybdenum sulfide (a-MoS_x) as HER catalyst as an alternative of Pt [221,222]. Photocathodes fabricated via spray deposition of a combination of a-MoS_x and TiO_2 on the BHJ layer obtained a photocurrent density of 200 $\mu A \cdot cm^{-2}$ at 0 V_{RHE} and up to 300 $\mu A \cdot cm^{-2}$ at –0.4 V_{RHE}. Another inorganic layer is TiO_x layer on P_3HT:PCBM BHJ layer and the catalytic film [223]. Moreover, metallic Al/Ti interfacial layers resulting in an enhancement in the photocurrent nearly about the 8 $mA \cdot cm^{-2}$ at 0 V vs. RHE. A 50-nm-thick C_{60} layer also functions as an interfacial layer, with a current density attaining 1 $mA \cdot cm^{-2}$ at 0 V vs. RHE [224]. Also, reduced graphene oxide, WO_3 and NiO, CuI, polyaniline underlayers are effective for persistent PEC features in acidic aqueous electrolytes [225–230]. The use of α-sexithiophene (α-6T) and chloroboron subphthalocyanine (SubPc) combined with C_{60} as the electron extracting layer gave more H_2 evolution [231]. MoS_3 coating gave 3 mW/cm^2 at 0 V vs. RHE [225]. Tandem cells are known to obtain high Open circuit voltage (Voc) in a solar cell. For water splitting, such high Voc is necessary, at least 1.23 V theoretically. Applications by the use of high Voc with the tandem structure are reported [231–238]. There are several review papers about using advanced organic and carbon-based materials [239–248], while the present paper focused only on the heterogeneous organic semiconductor photocatalysts.

Among these heterogeneous photocatalysts, the conjugated microporous polymers (CMPs) have been recognized as photocathodes for H_2 evolution from water to support a sacrificial electron donor. Sprick et al. also investigated various kinds of CMPs by varying monomer linker length and were investigated for photocatalytic H_2 evolution reactions [248]. Like CMPs, covalent organic frameworks (COFs) are also an emergent class of crystalline polymers comprised of organic units connected via covalent bonds to

produce porous networks. Very recently, Sick et al. reported first-time COFs as a new kinds of porous electrode materials of BDT-ETTA (benzo[1,2-b:4,5-b′]-dithiophene-2,6-dicarboxaldehyde (BDT); 1,1′,2,2′-tetra-p-aminophenylethylene, ETTA) for water-splitting reaction [249]. Further, these materials satisfy the necessities for light-driven water reduction application, which comprise effective light-harvesting, appropriate energy level positions, and stability.

6. Conclusions and Future Outlook

Energy harvesting technology from the limitless solar irradiation source has been recognized as a sustainable solution for the global energy crisis. In this review, the visible-light-driven water-splitting system has significantly improved since H_2 is a water-splitting reaction expected to support future societies. In this context, a series of heterogenous photocatalyst materials have been examined for PEC water splitting reaction. Special consideration has been paid to organophotocatalysts based electrodes for the applications of solar-driven water splitting reactions. (Oxy)nitrides, oxysulfides, and organophotocatalysts have the potential to acts as stable photoelectrodes for water redox reaction under visible-light illumination, have been shown to PEC behavior without noticeable degradation. In some cases, heterogenous semiconductor photocatalyst systems need to feature organophotocatalysts along with a simple conventional oxide and were evidenced to be effective for the stoichiometric decomposition of water into H_2 and O_2. Over the past few decades, the available photocatalysts for visible-light-driven water splitting has mostly comprised of metal oxides. The development of heterogenous photocatalysts attempting to attain the same role has probably given a boost to research on photocatalytic material for solar energy conversion.

In summary, over the past decades, (oxy)nitride and oxysulfides based photoelectrodes have been faced a high-speed advancement in terms of both the stable electrochemical nature as well as the activity of PEC water oxidation. Understanding the mechanism assembled by investigating this kind of photoanodes will cover a solid path for advancing other types of proficient photoanodes. In all these systems, the photoelectrode materials, which cannot merely contribute to the complete decomposition of water, can play active parts. The usage of these novel kinds of heterogeneous photocatalyst based materials and suitable electrocatalyst materials have more advantages in gathering solar energy. PEC water decomposition is already recognized as the most promising methodologies for obtaining solar hydrogen. In this perspective, developing new kinds of heterogeneous photocatalyst will be an efficient strategy for creating a commercially viable water-splitting system.

During the past few years, considerable research efforts have applied photoelectrochemistry for other reactions besides water splitting. In this context, the conversion of CO_2 into value-added organic molecules has gained enormous interest in recent years. Carbon dioxide reduction reaction (CO_2RR) is far more complicated than water splitting. Still, it permits the opportunity of extracting the greenhouse gas CO_2 from the atmosphere and turning it into value-added fuels. Commercially, products such as methane or ethanol generation via CO_2RR have been explored [250,251]. Conversely, the major limits for CO_2RR are finding suitable photoelectrodes and robust semiconductors to be kept in direct contact with the reaction, as the higher required reductive potentials (>1 V) improve materials corrosion [252,253]. Despite the described potentialities for the usage of photoelectrochemistry in H_2 production and CO_2RR, it has not been possible to demonstrate an application capable of competing economically with conventional procedures that are frequently used e.g., methane reforming permits obtaining H_2 at € 3/kg. In this regard, to be capable of developing alternate methods built on the usage of renewable energies such as photoelectrocatalysis, it is essential to promote efficient and robust devices created using cost-effective most-abundant electrode materials (like heterogeneous photocatalyst), demanding optimization approaches like the tandem arrangement of photoelectrodes to relax the stringent conditions required for effective PEC value-added solar fuel production.

Indeed, PEC water splitting development will help to identify and adapt photoelectrodes for other electrochemical reactions.

Author Contributions: P.A., M.A.G., A.M.A.-M., and K.N. Initiated and planned the subject and conceived the subject; P.A. perceived the subject, discussed related articles, wrote this manuscript collaboratively, and led this work. M.S.A. and R.J.R. assisted in writing. All authors have read and agreed to the published version of the manuscript.

Funding: The authors extend their appreciation to the Deputyship for Research and Innovation, "Ministry of Education" in Saudi Arabia for funding this research work through the Project number IFKSURP-025, Kingdom of Saudi Arabia.

Institutional Review Board Statement: Not applicable.

Informed Consent Statement: Not applicable.

Data Availability Statement: No new data were created or analyzed in this study. Data sharing is not applicable to this article.

Acknowledgments: The authors extend their appreciation to the Deputyship for Research and Innovation, "Ministry of Education" in Saudi Arabia for funding this research work through the Project number IFKSURP-025, Kingdom of Saudi Arabia.

Conflicts of Interest: The authors declare no conflict of interest.

References

1. Lewis, N.S.; Crabtree, G. *Basic Research Needs for Solar Energy Utilization: Report of the Basic Energy Sciences Workshop on Solar Energy Utilization, April 18–21, 2005*; US Department of Energy, Office of Basic Energy Science: Washington, DC, USA, 2005.
2. Walter, M.G.; Warren, E.L.; McKone, J.R.; Boettcher, S.W.; Mi, Q.; Santori, E.A.; Lewis, N.S. Solar water splitting cells. *Chem. Rev.* **2010**, *110*, 6446–6473. [CrossRef] [PubMed]
3. Herron, J.A.; Kim, J.; Upadhye, A.A.; Huber, G.W.; Maravelias, C.T. A general framework for the assessment of solar fuel technologies. *Energy Environ. Sci.* **2015**, *8*, 126–157. [CrossRef]
4. Lewis, N.S. Toward cost-effective solar energy use. *Science* **2007**, *315*, 798–801. [CrossRef] [PubMed]
5. Balzani, V.; Pacchioni, G.; Prato, M.; Zecchina, A. Solar-driven chemistry: Towards new catalytic solutions for a sustainable world. Rendiconti Lincei. *Sci. Fisiche E Nat.* **2019**, *30*, 443–452.
6. McKone, J.R.; Lewis, N.S.; Gray, H.B. Will solar-driven water-splitting devices see the light of day? *Chem. Mater.* **2014**, *26*, 407–414. [CrossRef]
7. Fujishima, A.; Honda, K. Electrochemical photolysis of water at a semiconductor electrode. *Nature* **1972**, *238*, 37–38. [CrossRef]
8. Xing, J.; Fang, W.Q.; Zhao, H.J.; Yang, H.G. Inorganic photocatalysts for overall water splitting. *Chem. Asian J.* **2012**, *7*, 642–657. [CrossRef]
9. Chen, X.; Shen, S.; Guo, L.; Mao, S.S. Semiconductor-based photocatalytic hydrogen generation. *Chem. Rev.* **2010**, *110*, 6503–6570. [CrossRef]
10. Lianos, P. Review of recent trends in photoelectrocatalytic conversion of solar energy to electricity and hydrogen. *Appl. Catal. B* **2017**, *210*, 235–254. [CrossRef]
11. Acar, C.; Dincer, I.; Zamfirescu, C. A review on selected heterogeneous photocatalysts for hydrogen production. *Int. J. Energy Res.* **2014**, *38*, 1903–1920. [CrossRef]
12. Arunachalam, P.; Al Mayouf, A.M. Photoelectrochemical Water Splitting. In *Noble Metal-Metal Oxide Hybrid Nanoparticles*; Woodhead Publishing: Cambridge, UK, 2019; pp. 585–606.
13. Jafari, T.; Moharreri, E.; Amin, A.S.; Miao, R.; Song, W.; Suib, S.L. Photocatalytic water splitting—The untamed dream: A review of recent advances. *Molecules* **2016**, *21*, 900. [CrossRef] [PubMed]
14. Ru Ng, A.Y.; Boruah, B.; Chin, K.F.; Modak, J.M.; Soo, H.S. Photoelectrochemical Cells for Artificial Photosynthesis: Alternatives to Water Oxidation. *ChemNanoMat* **2020**, *6*, 185–203. [CrossRef]
15. Deyab, N.M.; Salem, K.E.; Mokhtar, A.M.; Ramadan, M.; Steegstra, P.; Hubin, A.; Allam, N.K. Electrochemical Fabrication of Ternary Black Ti-Mo-Ni Oxide Nanotube Arrays for Enhanced Photoelectrochemical Water Oxidation. *ChemistrySelect* **2020**, *5*, 12151–12158. [CrossRef]
16. Tang, J.; Durrant, J.R.; Klug, D.R. Mechanism of photocatalytic water splitting in TiO_2. Reaction of water with photoholes, importance of charge carrier dynamics, and evidence for four-hole chemistry. *J. Am. Chem. Soc.* **2008**, *130*, 13885–13891. [CrossRef] [PubMed]
17. Kudo, A.; Miseki, Y. Heterogeneous photocatalyst materials for water splitting. *Chem. Soc. Rev.* **2009**, *38*, 253–278. [CrossRef]
18. Takata, T.; Hitoki, G.; Kondo, J.; Hara, M.; Kobayashi, H.; Domen, K. Visible-light-driven photocatalytic behavior of tantalum-oxynitride and nitride. *Res. Chem. Intermed.* **2007**, *33*, 13–25. [CrossRef]

19. Malathi, A.; Arunachalam, P.; Grace, A.N.; Madhavan, J.; Al-Mayouf, A.M. A robust visible-light driven BiFeWO6/BiOI nanohybrid with efficient photocatalytic and photoelectrochemical performance. *Appl. Surf. Sci.* **2017**, *412*, 85–95. [CrossRef]
20. Arunachalam, P.; Amer, M.S.; Ghanem, M.A.; Al-Mayouf, A.M.; Zhao, D. Activation effect of silver nanoparticles on the photoelectrochemical performance of mesoporous TiO_2 nanospheres photoanodes for water oxidation reaction. *Int. J. Hydrog. Energy* **2017**, *42*, 11346–11355. [CrossRef]
21. Amer, M.S.; Arunachalam, P.; Al-Mayouf, A.M.; Prasad, S.; Alshalwi, M.N.; Ghanem, M.A. Mesoporous tungsten trioxide photoanodes modified with nitrogen-doped carbon quantum dots for enhanced oxygen evolution photo-reaction. *Nanomaterials* **2019**, *9*, 1502. [CrossRef]
22. Grätzel, M. Photoelectrochemical cells. *Nature* **2001**, *414*, 338. [CrossRef]
23. Watanabe, T.; Fujishima, A.; Honda, K.-I. Photoelectrochemical reactions at SrTiO3 single crystal electrode. *Bull. Chem. Soc. Jpn.* **1976**, *49*, 355–358. [CrossRef]
24. Ghanem, M.A.; Arunachalam, P.; Amer, M.S.; Al-Mayouf, A.M. Mesoporous titanium dioxide photoanodes decorated with gold nanoparticles for boosting the photoelectrochemical alkali water oxidation. *Mater. Chem. Phys.* **2019**, *213*, 56–66. [CrossRef]
25. Melián, E.P.; López, C.R.; Méndez, A.O.; Díaz, O.G.; Suárez, M.N.; Rodríguez, J.D.; Navío, J.; Hevia, D.F. Hydrogen production using Pt-loaded TiO_2 photocatalysts. *Int. J. Hydrog. Energy* **2013**, *38*, 11737–11748. [CrossRef]
26. Yuan, Y.; Zhang, X.; Liu, L.; Jiang, X.; Lv, J.; Li, Z.; Zou, Z. Synthesis and photocatalytic characterization of a new photocatalyst $BaZrO_3$. *Int. J. Hydrog. Energy* **2008**, *33*, 5941–5946. [CrossRef]
27. Amer, M.S.; Ghanem, M.A.; Al-Mayouf, A.M.; Arunachalam, P.; Khdary, N.H. Low-loading of oxidized platinum nanoparticles into mesoporous titanium dioxide for effective and durable hydrogen evolution in acidic media. *Arab. J. Chem.* **2020**, *13*, 2257–2570. [CrossRef]
28. Amer, M.S.; Ghanem, M.A.; Al-Mayouf, A.M.; Arunachalam, P. Low-Symmetry Mesoporous Titanium Dioxide (lsm-TiO_2) Electrocatalyst for Efficient and Durable Oxygen Evolution in Aqueous Alkali. *J. Electrochem. Soc.* **2018**, *165*, H300–H309. [CrossRef]
29. Hara, Y.; Takashima, T.; Kobayashi, R.; Abeyrathna, S.; Ohtani, B.; Irie, H. Silver-inserted heterojunction photocatalyst consisting of zinc rhodium oxide and silver antimony oxide for overall pure-water splitting under visible light. *Appl. Catal. B Environ.* **2017**, *209*, 663–668. [CrossRef]
30. Amer, M.S.; Ghanem, M.A.; Arunachalam, P.; Al-Mayouf, A.M.; Hadadi, S.M. Bifunctional Electrocatalyst of Low-Symmetry Mesoporous Titanium Dioxide Modified with Cobalt Oxide for Oxygen Evolution and Reduction Reactions. *Catalysts* **2019**, *9*, 836. [CrossRef]
31. Hara, S.; Yoshimizu, M.; Tanigawa, S.; Ni, L.; Ohtani, B.; Irie, H. Hydrogen and oxygen evolution photocatalysts synthesized from strontium titanate by controlled doping and their performance in two-step overall water splitting under visible light. *J. Phys. Chem. C* **2011**, *116*, 17458–17463. [CrossRef]
32. Manikandan, M.; Tanabe, T.; Li, P.; Ueda, S.; Ramesh, G.V.; Kodiyath, R.; Ariga, K. Photocatalytic water splitting under visible light by mixed-valence Sn_3O_4. *ACS Appl. Mater. Interfaces* **2014**, *6*, 3790–3793. [CrossRef]
33. Kamimura, S.; Higashi, M.; Abe, R.; Ohno, T. Fabrication of a porous $ZnRh_2O_4$ photocathode for photoelectrochemical water splitting under visible light irradiation and a significant effect of surface modification by ZnO necking treatment. *J. Mater. Chem. A* **2016**, *4*, 6116–6123. [CrossRef]
34. Iwashina, K.; Iwase, A.; Nozawa, S.; Adachi, S.I.; Kudo, A. Visible-Light-Responsive CuLi1/3Ti_2/3O_2 Powders Prepared by a Molten CuCl Treatment of Li_2TiO_3 for Photocatalytic H_2 Evolution and Z-Schematic Water Splitting. *Chem. Mater.* **2016**, *28*, 4677–4685. [CrossRef]
35. Tateno, H.; Miseki, Y.; Sayama, K. Photoelectrochemical dimethoxylation of furan via a bromide redox mediator using a $BiVO_4/WO_3$ photoanode. *Chem. Commun.* **2017**, *53*, 4378–4381. [CrossRef] [PubMed]
36. Amano, F.; Li, D.; Ohtani, B. Fabrication and photoelectrochemical property of tungsten (VI) oxide films with a flake-wall structure. *Chem. Commun.* **2010**, *46*, 2769–2771. [CrossRef]
37. Hu, Y.-S.; Kleiman-Shwarsctein, A.; Stucky, G.D.; McFarland, E.W. Improved photoelectrochemical performance of Ti-doped α-Fe_2O_3 thin films by surface modification with fluoride. *Chem. Commun.* **2009**, 2652–2654. [CrossRef]
38. Sayama, K.; Nomura, A.; Zou, Z.; Abe, R.; Abe, Y.; Arakawa, H. Photoelectrochemical decomposition of water on nanocrystalline BiVO4 film electrodes under visible light. *Chem. Commun.* **2003**, 2908–2909. [CrossRef]
39. Shaddad, M.N.; Cardenas-Morcoso, D.; Arunachalam, P.; Garcia-Tecedor, M.; Ghanem, M.A.; Bisquert, J.; Al-Mayouf, A.; Gimenez, S. Enhancing the Optical Absorption and Interfacial Properties of $BiVO_4$ with Ag_3PO_4 Nanoparticles for Efficient Water Splitting. *J. Phys. Chem. C* **2018**, *122*, 11608–11615. [CrossRef]
40. Malathi, A.; Madhavan, J.; Ashokkumar, M.; Arunachalam, P. A review on $BiVO_4$ photocatalyst: Activity enhancement methods for solar photocatalytic applications. *Appl. Catal. A: Gen.* **2018**, *555*, 47–74.
41. Malathi, A.; Vasanthakumar, V.; Arunachalam, P.; Madhavan, J.; Ghanem, M.A. A low cost additive-free facile synthesis of BiFeWO6/BiVO4 nanocomposite with enhanced visible-light induced photocatalytic activity. *J. Colloid Interface Sci.* **2017**, *506*, 553–563. [CrossRef]
42. Hou, T.F.; Johar, M.A.; Boppella, R.; Hassan, M.A.; Patil, S.J.; Ryu, S.W.; Lee, D.W. Vertically aligned one-dimensional ZnO/V_2O_5 core-shell hetero-nanostructure for photoelectrochemical water splitting. *J. Energy Chem.* **2020**, *49*, 262–274. [CrossRef]

43. Ghosh, M.; Liu, J.; Chuang, S.S.; Jana, S.C. Fabrication of hierarchical V_2O_5 nanorods on TiO_2 nanofibers and their enhanced photocatalytic activity under visible light. *ChemCatChem* **2018**, *10*, 3305–3318. [CrossRef]
44. Ning, X.; Zhen, W.; Wu, Y.; Lu, G. Inhibition of CdS photocorrosion by Al_2O_3 shell for highly stable photocatalytic overall water splitting under visible light irradiation. *Appl. Catal. B Environ.* **2018**, *226*, 373–383. [CrossRef]
45. Li, F.; Zhao, W.; Leung, D.Y. Enhanced photoelectrocatalytic hydrogen production via Bi/$BiVO_4$ photoanode under visible light irradiation. *Appl. Catal. B Environ.* **2019**, *258*, 117954. [CrossRef]
46. Nagai, K.; Abe, T.; Kaneyasu, Y.; Yasuda, Y.; Kimishima, I.; Iyoda, T.; Imaya, H. A full-spectrum visible-light-responsive organophotocatalyst film for removal of trimethylamine. *ChemSusChem* **2011**, *4*, 727–730. [CrossRef]
47. Nagai, K.; Yasuda, Y.; Iyoda, T.; Abe, T. Multilayerization of Organophotocatalyst Films that Efficiently Utilize Natural Sunlight in a One-Pass-Flow Water Purification System. *ACS Sustain. Chem. Eng.* **2013**, *1*, 1033–1039. [CrossRef]
48. Mendori, D.; Hiroya, T.; Ueda, M.; Sanyoushi, M.; Nagai, K.; Abe, T. Novel photocatalytic material of organic p–n bilayer responsive to near-infrared energy. *Appl. Catal. B Environ.* **2017**, *205*, 514–518. [CrossRef]
49. Abe, T.; Tobinai, S.; Taira, N.; Chiba, J.; Itoh, T.; Nagai, K. Molecular hydrogen evolution by organic p/n bilayer film of phthalocyanine/fullerene in the entire visible-light energy region. *J. Phys. Chem. C* **2011**, *115*, 7701–7705. [CrossRef]
50. Abe, T.; Nagai, K.; Sekimoto, K.; Tajiri, A.; Norimatsu, T. Novel characteristics at a fullerene/water interface in an organic bilayer photoelectrode of phthalocyanine/fullerene. *Electrochem. Commun.* **2005**, *7*, 1129–1132. [CrossRef]
51. Abe, T.; Hiyama, Y.; Fukui, K.; Sahashi, K.; Nagai, K. Efficient p-zinc phthalocyanine/n-fullerene organic bilayer electrode for molecular hydrogen evolution induced by the full visible-light energy. *Int. J. Hydrog. Energy* **2015**, *40*, 9165–9170. [CrossRef]
52. Abe, T.; Nagai, K.; Kaneko, M.; Okubo, T.; Sekimoto, K.; Tajiri, A.; Norimatsu, T. A Novel and Efficient System of a Visible-Light-Responsive Organic Photoelectrocatalyst Working in a Water Phase. *ChemPhysChem* **2004**, *5*, 716–720. [CrossRef]
53. Zhang, S.; Sakai, R.; Abe, T.; Iyoda, T.; Norimatsu, T.; Nagai, K. Photoelectrochemical and photocatalytic properties of biphasic organic p-and n-type semiconductor nanoparticles fabricated by a reprecipitation process. *ACS Appl. Mater. Interfaces* **2011**, *3*, 1902–1909. [CrossRef] [PubMed]
54. Zhang, S.; Arunachalam, P.; Abe, T.; Iyoda, T.; Nagai, K. Photocatalytic decomposition of N-methyl-2-pyrrolidone, aldehydes, and thiol by biphase and p/n junction-like organic semiconductor composite nanoparticles responsive to nearly full spectrum of visible light. *J. Photochem. Photobiol. A Chem.* **2012**, *244*, 18–23. [CrossRef]
55. Arunachalam, P.; Zhang, S.; Abe, T.; Komura, M.; Iyoda, T.; Nagai, K. Weak visible light (mW/cm^2) organophotocatalysis for mineralization of amine, thiol and aldehyde by biphasic cobalt phthalocyanine/fullerene nanocomposites prepared by wet process. *Appl. Catal. B Environ.* **2016**, *193*, 240–247. [CrossRef]
56. Kasai, H.; Nalwa, H.S.; Oikawa, H.; Okada, S.; Matsuda, H.; Minami, N.; Kakuta, A.; Ono, K.; Mukoh, A.; Nakanishi, H. A novel preparation method of organic microcrystals. *Jpn. J. Appl. Phys.* **1992**, *31*, L1132. [CrossRef]
57. Tachikawa, T.; Chung, H.R.; Masuhara, A.; Kasai, H.; Oikawa, H.; Nakanishi, H.; Fujitsuka, M.; Majima, T. In situ and ex situ observations of the growth dynamics of single perylene nanocrystals in water. *J. Am. Chem. Soc.* **2006**, *128*, 15944–15945. [CrossRef]
58. Baba, K.; Kasai, H.; Nishida, K.; Nakanishi, H. Poly (N-isopropylacrylamide)-based thermoresponsive behavior of fluorescent organic nanocrystals. *Jpn. J. Appl. Phys.* **2011**, *50*, 010202. [CrossRef]
59. Asahi, R.; Morikawa, T.; Ohwaki, T.; Aoki, K.; Taga, Y. Visible-light photocatalysis in nitrogen-doped titanium oxides. *Science* **2001**, *293*, 269–271. [CrossRef]
60. Hitoki, G.; Takata, T.; Kondo, J.; Hara, M.; Kobayashi, H.; Domen, K. (Oxy) nitrides as new photocatalysts for water splitting under visible light irradiation. *Electrochemistry* **2002**, *70*, 463–465. [CrossRef]
61. Abe, R.; Takata, T.; Sugihara, H.; Domen, K. The use of TiCl4 treatment to enhance the photocurrent in a TaON photoelectrode under visible light irradiation. *Chem. Lett.* **2005**, *34*, 1162–1163. [CrossRef]
62. Mucha, N.R.; Som, J.; Choi, J.; Shaji, S.; Gupta, R.K.; Meyer, H.M.; Kumar, D. High-Performance Titanium Oxynitride Thin Films for Electrocatalytic Water Oxidation. *ACS Appl. Energy Mater.* **2020**, *3*, 8366–8374. [CrossRef]
63. Nishimura, N.; Raphael, B.; Maeda, K.; Le Gendre, L.; Abe, R.; Kubota, J.; Domen, K. Effect of TiCl4 treatment on the photoelectrochemical properties of LaTiO2N electrodes for water splitting under visible light. *Thin Solid Film.* **2010**, *518*, 5855–5859. [CrossRef]
64. Abe, T.; Nagai, K.; Sekimoto, K.; Tajiri, A.; Norimatsu, T. Novel photocathodic characteristics of organic bilayer composed of a phthalocyanine and a perylene derivative in a water phase containing a redox molecule. *J. Electroanal. Chem.* **2005**, *583*, 327–332. [CrossRef]
65. Abe, T.; Nagai, K.; Ichinohe, H.; Shibata, T.; Tajiri, A.; Norimatsu, T. An efficient oxidation at photofunctional interface of phthalocyanine in combination with fullerene. *J. Electroanal. Chem.* **2007**, *599*, 65–71. [CrossRef]
66. Gerischer, H.; Luebke, M. Competition between Photocorrosion and Photooxidation of Redox Systems at n-Type Semiconductor Electrodes. *Ber. Der Bunsenges. Für Phys. Chem.* **1983**, *87*, 123–128. [CrossRef]
67. Balaz, S.; Porter, S.H.; Woodward, P.M.; Brillson, L.J. Electronic structure of tantalum oxynitride perovskite photocatalysts. *Chem. Mater.* **2013**, *25*, 3337–3343. [CrossRef]
68. Zhang, P.; Zhang, J.; Gong, J. Tantalum-based semiconductors for solar water splitting. *Chem. Soc. Rev.* **2014**, *43*, 4395–4422. [CrossRef]

69. Hara, M.; Hitoki, G.; Takata, T.; Kondo, J.N.; Kobayashi, H.; Domen, K. TaON and Ta3N5 as new visible light driven photocatalysts. *Catal. Today* **2003**, *78*, 555–560. [CrossRef]
70. Hitoki, G.; Takata, T.; Kondo, J.N.; Hara, M.; Kobayashi, H.; Domen, K. An oxynitride, TaON, as an efficient water oxidation photocatalyst under visible light irradiation ($\lambda \leq 500$ nm). *Chem. Commun.* **2002**, 1698–1699. [CrossRef]
71. Hitoki, G.; Ishikawa, A.; Takata, T.; Kondo, J.N.; Hara, M.; Domen, K. Ta3N5 as a novel visible light-driven photocatalyst ($\lambda < 600$ nm). *Chem. Lett.* **2002**, *31*, 736–737.
72. Kaneko, M.; Fujii, M.; Hisatomi, T.; Yamashita, K.; Domen, K. Regression model for stabilization energies associated with anion ordering in perovskite-type oxynitrides. *J. Energy Chem.* **2019**, *36*, 7–14. [CrossRef]
73. Kawashima, K.; Hojamberdiev, M.; Yubuta, K.; Domen, K.; Teshima, K. Synthesis and visible-light-induced sacrificial photocatalytic water oxidation of quinary oxynitride BaNb0. 5Ta0. 5O2N crystals. *J. Energy Chem.* **2018**, *27*, 1415–1421. [CrossRef]
74. Takata, T.; Pan, C.; Domen, K. Recent progress in oxynitride photocatalysts for visible-light-driven water splitting. *Sci. Technol. Adv. Mater.* **2015**, *16*, 033506. [CrossRef] [PubMed]
75. Fang, C.; Orhan, E.; De Wijs, G.; Hintzen, H.; De Groot, R.; Marchand, R.; Saillard, J.Y. The electronic structure of tantalum (oxy) nitrides TaON and Ta3N5. *J. Mater. Chem.* **2001**, *11*, 1248–1252. [CrossRef]
76. Fang, C.; De Wijs, G.; Orhan, E.; De With, G.; De Groot, R.; Hintzen, H.; Marchand, R. Local structure and electronic properties of BaTaO2N with perovskite-type structure. *J. Phys. Chem. Solids* **2003**, *64*, 281–286. [CrossRef]
77. Sakar, M.; Prakash, R.M.; Shinde, K.; Balakrishna, G.R. Revisiting the materials and mechanism of metal oxynitrides for photocatalysis. *Int. J. Hydrog. Energy* **2020**, *45*, 7691–7705. [CrossRef]
78. Maeda, K.; Domen, K. New non-oxide photocatalysts designed for overall water splitting under visible light. *J. Phys. Chem. C* **2007**, *111*, 7851–7861. [CrossRef]
79. Amano, F.; Ishinaga, E.; Yamakata, A. Effect of particle size on the photocatalytic activity of WO3 particles for water oxidation. *J. Phys. Chem. C* **2013**, *117*, 22584–22590. [CrossRef]
80. Kawashima, K.; Hojamberdiev, M.; Wagata, H.; Yubuta, K.; Vequizo, J.J.M.; Yamakata, A.; Oishi, S.; Domen, K.; Teshima, K. NH3-assisted flux mediated direct growth of $LaTiO_2N$ crystallites for visible-light-induced water splitting. *J. Phys. Chem. C* **2015**, *119*, 15896–15904. [CrossRef]
81. Abeysinghe, D.; Skrabalak, S.E. Toward shape-controlled metal oxynitride and nitride particles for solar energy applications. *ACS Energy Lett.* **2018**, *3*, 1331–1344. [CrossRef]
82. Maegli, A.E.; Pokrant, S.; Hisatomi, T.; Trottmann, M.; Domen, K.; Weidenkaff, A. Enhancement of photocatalytic water oxidation by the morphological control of LaTiO2N and cobalt oxide catalysts. *J. Phys. Chem. C* **2014**, *118*, 16344–16351. [CrossRef]
83. Kodera, M.; Katayama, M.; Hisatomi, T.; Minegishi, T.; Domen, K. Effects of flux treatment on morphology of single-crystalline $BaNbO_2N$ particles. *CrystEngComm* **2016**, *18*, 3186–3190. [CrossRef]
84. Hojamberdiev, M.; Kawashima, K.; Hisatomi, T.; Katayama, M.; Hasegawa, M.; Domen, K.; Teshima, K. Distinguishing the effects of altered morphology and size on the visible light-induced water oxidation activity and photoelectrochemical performance of $BaTaO_2N$ crystal structures. *Faraday Discuss.* **2019**, *215*, 227–241. [CrossRef] [PubMed]
85. Hirayama, N.; Nakata, H.; Wakayama, H.; Nishioka, S.; Kanazawa, T.; Kamata, R.; Ebato, Y.; Kosaku, K.; Kumagai, H.; Yamakata, A.; et al. Solar-Driven Photoelectrochemical Water Oxidation over an n-Type Lead–Titanium Oxyfluoride Anode. *J. Am. Chem. Soc.* **2019**, *141*, 17158–17165. [CrossRef] [PubMed]
86. Lawley, C.; Nachtegaal, M.; Stahn, J.; Roddatis, V.; Döbeli, M.; Schmidt, T.J.; Lippert, T. Examining the surface evolution of $LaTiO_xN_y$ an oxynitride solar water splitting photocatalyst. *Nat. Commun.* **2020**, *11*, 1728. [CrossRef]
87. Wang, X.; Maeda, K.; Lee, Y.; Domen, K. Enhancement of photocatalytic activity of (Zn1 + xGe)(N_2O_x) for visible-light-driven overall water splitting by calcination under nitrogen. *Chem. Phys. Lett.* **2008**, *457*, 134–136. [CrossRef]
88. Maeda, K.; Teramura, K.; Lu, D.; Takata, T.; Saito, N.; Inoue, Y.; Domen, K. Photocatalyst releasing hydrogen from water. *Nature* **2006**, *440*, 295. [CrossRef]
89. Ishikawa, A.; Takata, T.; Kondo, J.N.; Hara, M.; Domen, K. Electrochemical behavior of thin Ta3N5 semiconductor film. *J. Phys. Chem. B* **2004**, *108*, 11049–11053. [CrossRef]
90. Le Paven-Thivet, C.; Ishikawa, A.; Ziani, A.; Le Gendre, L.; Yoshida, M.; Kubota, J.; Tessier, F.; Domen, K. Photoelectrochemical properties of crystalline perovskite lanthanum titanium oxynitride films under visible light. *J. Phys. Chem. C* **2009**, *113*, 6156–6162. [CrossRef]
91. Konta, R.; Ishii, T.; Kato, H.; Kudo, A. Photocatalytic activities of noble metal ion doped $SrTiO_3$ under visible light irradiation. *J. Phys. Chem. B* **2004**, *108*, 8992–8995. [CrossRef]
92. Kato, H.; Asakura, K.; Kudo, A. Highly efficient water splitting into H_2 and O_2 over lanthanum-doped $NaTaO_3$ photocatalysts with high crystallinity and surface nanostructure. *J. Am. Chem. Soc.* **2003**, *125*, 3082–3089. [CrossRef]
93. Feng, X.; LaTempa, T.J.; Basham, J.I.; Mor, G.K.; Varghese, O.K.; Grimes, C.A. Ta_3N_5 nanotube arrays for visible light water photoelectrolysis. *Nano Lett.* **2010**, *10*, 948–952. [CrossRef] [PubMed]
94. Si, W.; Pergolesi, D.; Haydous, F.; Fluri, A.; Wokaun, A.; Lippert, T. Investigating the behavior of various cocatalysts on LaTaON 2 photoanode for visible light water splitting. *Phys. Chem. Chem. Phys.* **2017**, *19*, 656–662. [CrossRef]
95. Lin, G.; Wang, R.; Cao, T.; Yuan, L.; Xu, X. Zr modified $SrNbO_2N$ as active photocatalyst for water oxidation under visible light illumination. *Inorg. Chem. Front.* **2020**, *7*, 2629–2636. [CrossRef]

96. Oka, D.; Hirose, Y.; Kaneko, M.; Nakao, S.; Fukumura, T.; Yamashita, K.; Hasegawa, T. Anion-Substitution-Induced Nonrigid Variation of Band Structure in $SrNbO_3$–x N x (0 ≤ x ≤ 1) Epitaxial Thin Films. *ACS Appl. Mater. Interfaces* **2018**, *10*, 35008–35015. [CrossRef] [PubMed]
97. Sun, X.; Liu, G.; Xu, X. Defect management and efficient photocatalytic water oxidation reaction over Mg modified SrNbO 2 N. *J. Mater. Chem. A* **2018**, *6*, 10947–10957. [CrossRef]
98. Hisatomi, T.; Katayama, C.; Moriya, Y.; Minegishi, T.; Katayama, M.; Nishiyama, H.; Yamada, T.; Domen, K. Photocatalytic oxygen evolution using $BaNbO_2N$ modified with cobalt oxide under photoexcitation up to 740 nm. *Energy Environ. Sci.* **2013**, *6*, 3595–3599. [CrossRef]
99. Arunachalam, P.; Shaddad, M.N.; Ghanem, M.A.; Al-Mayouf, A.M.; Weller, M.T. Zinc tantalum Oxynitride (ZnTaO2N) photoanode modified with cobalt phosphate layers for the photoelectrochemical oxidation of alkali water. *Nanomaterials* **2018**, *8*, 48. [CrossRef] [PubMed]
100. Landsmann, S.; Maegli, A.E.; Trottmann, M.; Battaglia, C.; Weidenkaff, A.; Pokrant, S. Design guidelines for high-performance particle-based photoanodes for water splitting: Lanthanum titanium oxynitride as a model. *ChemSusChem* **2015**, *8*, 3451–3458. [CrossRef]
101. Wang, J.; Wang, X.; Liu, B.; Li, X.; Cao, M. Facile synthesis of $SrNbO_2N$ nanoparticles with excellent visible-light photocatalytic performances. *Mater. Lett.* **2015**, *152*, 131–134. [CrossRef]
102. Li, Y.; Nagato, K.; Delaunay, J.-J.; Kubota, J.; Domen, K. Fabrication of highly ordered Ta2O5 and Ta3N5 nanorod arrays by nanoimprinting and through-mask anodization. *Nanotechnology* **2013**, *25*, 014013. [CrossRef]
103. Li, Y.; Takata, T.; Cha, D.; Takanabe, K.; Minegishi, T.; Kubota, J.; Domen, K. Vertically Aligned Ta3N5 Nanorod Arrays for Solar-Driven Photoelectrochemical Water Splitting. *Adv. Mater.* **2013**, *25*, 125–131. [CrossRef] [PubMed]
104. Li, Y.; Zhang, L.; Torres-Pardo, A.; González-Calbet, J.M.; Ma, Y.; Oleynikov, P.; Terasaki, O.; Asahina, S.; Shima, M.; Cha, D. Cobalt phosphate-modified barium-doped tantalum nitride nanorod photoanode with 1.5% solar energy conversion efficiency. *Nat. Commun.* **2013**, *4*, 2566. [CrossRef] [PubMed]
105. Higashi, M.; Domen, K.; Abe, R. Fabrication of efficient TaON and Ta3N5 photoanodes for water splitting under visible light irradiation. *Energy Environ. Sci.* **2011**, *4*, 4138–4147. [CrossRef]
106. Higashi, M.; Domen, K.; Abe, R. Highly stable water splitting on oxynitride TaON photoanode system under visible light irradiation. *J. Am. Chem. Soc.* **2012**, *134*, 6968–6971. [CrossRef] [PubMed]
107. Theerthagiri, J.; Thiagarajan, K.; Senthilkumar, B.; Khan, Z.; Senthil, R.A.; Arunachalam, P.; Ashokkumar, M. Synthesis of hierarchical cobalt phosphate nanoflakes and their enhanced electrochemical performances for supercapacitor applications. *ChemistrySelect* **2017**, *2*, 201–210. [CrossRef]
108. Duraisamy, N.; Arshid, N.; Kandiah, K.; Iqbal, J.; Arunachalam, P.; Dhanaraj, G.; Ramesh, S. Development of asymmetric device using Co 3 (PO 4) 2 as a positive electrode for energy storage application. *J. Mater. Sci. Mater. Electron.* **2019**, *30*, 7435–7446. [CrossRef]
109. Haydous, F.; Si, W.; Guzenko, V.A.; Waag, F.; Pomjakushina, E.; El Kazzi, M.; Lippert, T. Improved Photoelectrochemical Water Splitting of $CaNbO_2N$ Photoanodes by CoPi Photodeposition and Surface Passivation. *J. Phys. Chem. C* **2018**, *123*, 1059–1068. [CrossRef]
110. Abe, R.; Higashi, M.; Domen, K. Facile fabrication of an efficient oxynitride TaON photoanode for overall water splitting into H_2 and O_2 under visible light irradiation. *J. Am. Chem. Soc.* **2010**, *132*, 11828–11829. [CrossRef]
111. Hisatomi, T.; Katayama, C.; Teramura, K.; Takata, T.; Moriya, Y.; Minegishi, T.; Katayama, M.; Nishiyama, H.; Yamada, T.; Domen, K. The effects of preparation conditions for a BaNbO2N photocatalyst on its physical properties. *ChemSusChem* **2014**, *7*, 2016–2021. [CrossRef]
112. Zhang, F.; Yamakata, A.; Maeda, K.; Moriya, Y.; Takata, T.; Kubota, J.; Teshima, K.; Oishi, S.; Domen, K. Cobalt-modified porous single-crystalline LaTiO2N for highly efficient water oxidation under visible light. *J. Am. Chem. Soc.* **2012**, *134*, 8348–8351. [CrossRef]
113. Yokoyama, D.; Hashiguchi, H.; Maeda, K.; Minegishi, T.; Takata, T.; Abe, R.; Kubota, J.; Domen, K. Ta3N5 photoanodes for water splitting prepared by sputtering. *Thin Solid Film.* **2011**, *519*, 2087–2092. [CrossRef]
114. Zhang, L.; Song, Y.; Feng, J.; Fang, T.; Zhong, Y.; Li, Z.; Zou, Z. Photoelectrochemical water oxidation of $LaTaON_2$ under visible-light irradiation. *Int. J. Hydrog. Energy* **2014**, *39*, 7697–7704. [CrossRef]
115. Black, A.P.; Suzuki, H.; Higashi, M.; Frontera, C.; Ritter, C.; De, C.; Fuertes, A. New rare earth hafnium oxynitride perovskites with photocatalytic activity in water oxidation and reduction. *Chem. Commun.* **2018**, *54*, 1525–1528. [CrossRef] [PubMed]
116. Takata, T.; Pan, C.; Domen, K. Design and development of oxynitride photocatalysts for overall water splitting under visible light irradiation. *ChemElectroChem* **2016**, *3*, 31–37. [CrossRef]
117. Siritanaratkul, B.; Maeda, K.; Hisatomi, T.; Domen, K. Synthesis and Photocatalytic Activity of Perovskite Niobium Oxynitrides with Wide Visible-Light Absorption Bands. *ChemSusChem* **2011**, *4*, 74–78. [CrossRef]
118. Maeda, K.; Higashi, M.; Siritanaratkul, B.; Abe, R.; Domen, K. $SrNbO_2N$ as a water-splitting photoanode with a wide visible-light absorption band. *J. Am. Chem. Soc.* **2011**, *133*, 12334–12337. [CrossRef]
119. Arunachalam, P.; Al-Mayouf, A.; Ghanem, M.A.; Shaddad, M.N.; Weller, M.T. Photoelectrochemical oxidation of water using La(Ta, Nb)O2N modified electrodes. *Int. J. Hydrog. Energy* **2016**, *41*, 11644–11652. [CrossRef]

120. Shaddad, M.N.; Arunachalam, P.; Al-Mayouf, A.M.; Ghanem, M.A.; Alharthi, A.I. Enhanced photoelectrochemical oxidation of alkali water over cobalt phosphate (Co-Pi) catalyst-modified $ZnLaTaON_2$ photoanodes. *Ionics* **2018**, *25*, 737–745. [CrossRef]
121. Walsh, D.; Sanchez-Ballester, N.M.; Ting, V.P.; Hall, S.R.; Terry, L.R.; Weller, M.T. Visible light promoted photocatalytic water oxidation: Effect of metal oxide catalyst composition and light intensity. *Catal. Sci. Technol.* **2015**, *5*, 4760–4764. [CrossRef]
122. Kanan, M.W.; Nocera, D.G. In situ formation of an oxygen-evolving catalyst in neutral water containing phosphate and Co^{2+}. *Science* **2008**, *321*, 1072–1075. [CrossRef]
123. Al-Sharif, M.S.; Arunachalam, P.; Abiti, T.; Amer, M.S.; Al-Shalwi, M.; Ghanem, M.A. Mesoporous cobalt phosphate electrocatalyst prepared using liquid crystal template for methanol oxidation reaction in alkaline solution. *Arab. J. Chem.* **2020**, *13*, 2873–2882. [CrossRef]
124. Zhen, C.; Wang, L.; Liu, G.; Lu, G.Q.M.; Cheng, H.-M. Template-free synthesis of Ta3N5 nanorod arrays for efficient photoelectrochemical water splitting. *Chem. Commun.* **2013**, *49*, 3019–3021. [CrossRef] [PubMed]
125. Roy, P.; Berger, S.; Schmuki, P. TiO_2 nanotubes: Synthesis and applications. *Angew. Chem. Int. Ed.* **2011**, *50*, 2904–2939. [CrossRef] [PubMed]
126. Song, F.; Hu, X. Exfoliation of layered double hydroxides for enhanced oxygen evolution catalysis. *Nat. Commun.* **2014**, *5*, 4477. [CrossRef] [PubMed]
127. Gong, M.; Li, Y.; Wang, H.; Liang, Y.; Wu, J.Z.; Zhou, J.; Wang, J.; Regier, T.; Wei, F.; Dai, H. An advanced Ni–Fe layered double hydroxide electrocatalyst for water oxidation. *J. Am. Chem. Soc.* **2013**, *135*, 8452–8455. [CrossRef]
128. Shao, M.; Ning, F.; Wei, M.; Evans, D.G.; Duan, X. Hierarchical nanowire arrays based on ZnO core-layered double hydroxide shell for largely enhanced photoelectrochemical water splitting. *Adv. Funct. Mater.* **2014**, *24*, 580–586. [CrossRef]
129. Wang, L.; Dionigi, F.; Nguyen, N.T.; Kirchgeorg, R.; Gliech, M.; Grigorescu, S.; Strasser, P.; Schmuki, P. Tantalum nitride nanorod arrays: Introducing Ni–Fe layered double hydroxides as a cocatalyst strongly stabilizing photoanodes in water splitting. *Chem. Mater.* **2015**, *27*, 2360–2366. [CrossRef]
130. Liao, M.; Feng, J.; Luo, W.; Wang, Z.; Zhang, J.; Li, Z.; Yu, T.; Zou, Z. Co_3O_4 nanoparticles as robust water oxidation catalysts towards remarkably enhanced photostability of a Ta3N5 photoanode. *Adv. Funct. Mater.* **2012**, *22*, 3066–3074. [CrossRef]
131. Allam, N.K.; Poncheri, A.J.; El-Sayed, M.A. Vertically oriented Ti–Pd mixed oxynitride nanotube arrays for enhanced photoelectrochemical water splitting. *ACS Nano* **2011**, *5*, 5056–5066. [CrossRef]
132. Chen, X.; Burda, C. Photoelectron spectroscopic investigation of nitrogen-doped titania nanoparticles. *J. Phys. Chem. B* **2004**, *108*, 15446–15449. [CrossRef]
133. Kim, D.; Fujimoto, S.; Schmuki, P.; Tsuchiya, H. Nitrogen doped anodic TiO_2 nanotubes grown from nitrogen-containing Ti alloys. *Electrochem. Commun.* **2008**, *10*, 910–913. [CrossRef]
134. Soliman, K.A.; Zedan, A.F.; Khalifa, A.; El-Sayed, H.A.; Aljaber, A.S.; AlQaradawi, S.Y.; Allam, N.K. Silver nanoparticles-decorated titanium oxynitride nanotube arrays for enhanced solar fuel generation. *Sci. Rep.* **2017**, *7*, 1913. [CrossRef] [PubMed]
135. Ce'line, M.L.; Alexandra, E.M.; Kevin, S.; Takashi, H.; Nicolas, X.; Eugenio, H.O.; Songhak, Y.; Anke, W.; Rosendo, S.; Michael, G. $LaTiO_2N/In_2O_3$ photoanodes with improved performance for solar water splitting. *Chem. Commun.* **2012**, *48*, 820–882.
136. Gujral, S.S.; Simonov, A.; Higashi, M.; Fang, X.; Abe, R.; Spiccia, L. Highly Dispersed Cobalt Oxide on TaON as Efficient Photoanodes for Long-Term Solar Water Splitting. *ACS Catal.* **2016**, *6*, 3404–3417. [CrossRef]
137. Higashi, M.; Domen, K.; Abe, R. Fabrication of an Efficient $BaTaO_2N$ Photoanode Harvesting a Wide Range of Visible Light for Water Splitting. *J. Am. Chem. Soc.* **2013**, *135*, 10238–10241. [CrossRef]
138. Seo, J.; Hisatomi, T.; Nakabayashi, M.; Shibata, N.; Minegishi, T.; Katayama, M.; Domen, K. Efficient Solar-Driven Water Oxidation over Perovskite-Type BaNbO2N Photoanodes Absorbing Visible Light up to 740 nm. *Adv. Energy Mater.* **2018**, *8*, 1800094. [CrossRef]
139. Urabe, H.; Hisatomi, T.; Minegishi, T.; Kubota, J.; Domen, K. Photoelectrochemical Properties of $SrNbO_2N$ Photoanodes for Water Oxidation Fabricated by the Particle Transfer Method. *Faraday Discuss.* **2014**, *176*, 213–223. [CrossRef]
140. Ueda, K.; Minegishi, T.; Clune, J.; Nakabayashi, M.; Hisatomi, T.; Nishiyama, H.; Katayama, M.; Shibata, N.; Kubota, J.; Yamada, T.; et al. Photoelectrochemical Oxidation of Water Using $BaTaO_2N$ Photoanodes Prepared by Particle Transfer Method. *J. Am. Chem. Soc.* **2015**, *137*, 2227–2230. [CrossRef]
141. Kodera, M.; Urabe, H.; Katayama, M.; Hisatomi, T.; Minegishi, T.; Domen, K. Effects of Flux Synthesis on $SrNbO_2N$ Particles for Photoelectrochemical Water Splitting. *J. Mater. Chem. A* **2016**, *4*, 7658–7664. [CrossRef]
142. Seo, J.; Nakabayashi, M.; Hisatomi, T.; Shibata, N.; Minegishi, T.; Katayama, M.; Domen, K. The effects of annealing barium niobium oxynitride in argon on photoelectrochemical water oxidation activity. *J. Mater. Chem. A* **2019**, *7*, 493–502. [CrossRef]
143. Zili, M.; Aleksander, J.; Janine, G.; Anna, R.; Thomas, T.; Tetyana, M.B.; Geoffroy, H.; Andrew, J.P.; Richar, D.; Piotr, K.; et al. Exploring the Origins of Improved Photocurrent by Acidic Treatment for Quaternary Tantalum-based Oxynitride Photoanodes on the Example of $CaTaO_2N$. *J. Phys. Chem. C* **2020**, *124*, 152–160.
144. Maoqi, C.; Hongmei, L.; Kang, L.; Junhua, H.; Hao, P.; Junwei, F.; Min, L. Vertical $SrNbO_2N$ Nanorod Arrays for Solar-Driven Photoelectrochemical Water Splitting. *Solar RRL* **2020**, 202000448. [CrossRef]
145. Yingchen, Y.; Zirui, L.; Weisheng, L.; Yichen, W.; Rong, L.; Chao, Q.; Liping, Z. Enhanced photoelectrochemical water-splitting performance of $SrNbO_2N$ photoanodes using flux-assisted synthesis method and surface defect management. *Sustain. Energy Fuels* **2020**, *4*, 1674–1680.

146. Ishikawa, A.; Takata, T.; Kondo, J.N.; Hara, M.; Kobayashi, H.; Domen, K. Oxysulfide $Sm2Ti_2S_2O_5$ as a stable photocatalyst for water oxidation and reduction under visible light irradiation ($\lambda \leq 650$ nm). *J. Am. Chem. Soc.* **2002**, *124*, 13547–13553. [CrossRef]
147. Ishikawa, A.; Yamada, Y.; Takata, T.; Kondo, J.N.; Hara, M.; Kobayashi, H.; Domen, K. Novel synthesis and photocatalytic activity of oxysulfide $Sm2Ti_2S_2O_5$. *Chem. Mater.* **2003**, *15*, 4442–4446. [CrossRef]
148. Williams, R. Becquerel photovoltaic effect in binary compounds. *J. Chem. Phys.* **1960**, *32*, 1505–1514. [CrossRef]
149. Ellis, A.B.; Kaiser, S.W.; Bolts, J.M.; Wrighton, M.S. Study of n-type semiconducting cadmium chalcogenide-based photoelectrochemical cells employing polychalcogenide electrolytes. *J. Am. Chem. Soc.* **1977**, *99*, 2839–2848. [CrossRef]
150. Harriman, A.; Thomas, J.; Milward, G. Catalytic and structural properties of iridium-iridium dioxide colloids. *New J. Chem.* **1987**, *11*, 757–762.
151. Harriman, A.; Pickering, I.J.; Thomas, J.M.; Christensen, P.A. Metal oxides as heterogeneous catalysts for oxygen evolution under photochemical conditions. *J. Chem. Soc. Faraday Trans. 1 Phys. Chem. Condens. Phases* **1988**, *84*, 2795–2806. [CrossRef]
152. Ma, G.; Chen, S.; Kuang, Y.; Akiyama, S.; Hisatomi, T.; Nakabayashi, M.; Shibata, N.; Katayama, M.; Minegishi, T.; Domen, K. Visible light-driven Z-scheme water splitting using oxysulfide H2 evolution photocatalysts. *J. Phys. Chem. Lett.* **2016**, *7*, 3892–3896. [CrossRef]
153. Ishikawa, A.; Takata, T.; Matsumura, T.; Kondo, J.N.; Hara, M.; Kobayashi, H.; Domen, K. Oxysulfides $Ln_2Ti_2S_2O_5$ as stable photocatalysts for water oxidation and reduction under visible-light irradiation. *J. Phys. Chem. B* **2004**, *108*, 2637–2642. [CrossRef]
154. Zhang, F.; Maeda, K.; Takata, T.; Domen, K. Modification of oxysulfides with two nanoparticulate cocatalysts to achieve enhanced hydrogen production from water with visible light. *Chem. Commun.* **2010**, *46*, 7313–7315. [CrossRef] [PubMed]
155. Ogisu, K.; Ishikawa, A.; Teramura, K.; Toda, K.; Hara, M.; Domen, K. Lanthanum–indium oxysulfide as a visible light driven photocatalyst for water splitting. *Chem. Lett.* **2007**, *36*, 854–855. [CrossRef]
156. Ogisu, K.; Ishikawa, A.; Shimodaira, Y.; Takata, T.; Kobayashi, H.; Domen, K. Electronic band structures and photochemical properties of La−Ga-based oxysulfides. *J. Phys. Chem. C* **2008**, *112*, 11978–11984. [CrossRef]
157. Liu, J.; Hisatomi, T.; Ma, G.; Iwanaga, A.; Minegishi, T.; Moriya, Y.; Katayama, M.; Kubota, J.; Domen, K. Improving the photoelectrochemical activity of $La_5Ti_2CuS_5O_7$ for hydrogen evolution by particle transfer and doping. *Energy Environ. Sci.* **2014**, *7*, 2239–2242. [CrossRef]
158. Ma, G.; Suzuki, Y.; Singh, R.B.; Iwanaga, A.; Moriya, Y.; Minegishi, T.; Liu, J.; Hisatomi, T.; Nishiyama, H.; Katayama, M. Photoanodic and photocathodic behaviour of $La_5Ti_2Cu_5O_7$ electrodes in the water splitting reaction. *Chem. Sci.* **2015**, *6*, 4513–4518. [CrossRef]
159. Hisatomi, T.; Okamura, S.; Liu, J.; Shinohara, Y.; Ueda, K.; Higashi, T.; Katayama, M.; Minegishi, T.; Domen, K. $La_5Ti_2Cu_{1-x}AgxS_5O_7$ photocathodes operating at positive potentials during photoelectrochemical hydrogen evolution under irradiation of up to 710 nm. *Energy Environ. Sci.* **2015**, *8*, 3354–3362. [CrossRef]
160. Yoshimizu, M.; Kobayashi, R.; Saegusa, M.; Takashima, T.; Funakubo, H.; Akiyama, K.; Yoshihisa, M.; Irie, H. Photocatalytic hydrogen evolution over β-iron silicide under infrared-light irradiation. *Chem. Commun.* **2015**, *51*, 2818–2820. [CrossRef]
161. Akiyama, K.; Motoizumi, Y.; Funakubo, H.; Irie, H.; Matsumoto, Y. Metal–organic chemical vapor deposition growth of β-FeSi2/Si composite powder via vapor–liquid–solid method and its photocatalytic properties. *Jpn. J. Appl. Phys.* **2016**, *55*, 06HC02. [CrossRef]
162. Akiyama, K.; Motoizumi, Y.; Okuda, T.; Funakubo, H.; Irie, H.; Matsumoto, Y. Synthesis and Photocatalytic Properties of Iron Disilicide/SiC Composite Powder. *MRS Adv.* **2017**, *2*, 471–476. [CrossRef]
163. Wang, X.; Maeda, K.; Thomas, A.; Takanabe, K.; Xin, G.; Carlsson, J.M.; Domen, K.; Antonietti, M. A metal-free polymeric photocatalyst for hydrogen production from water under visible light. *Nat. Mater.* **2009**, *8*, 76–80. [CrossRef] [PubMed]
164. Liu, J.; Liu, Y.; Liu, N.; Han, Y.; Zhang, X.; Huang, H.; Lifshitz, Y.; Lee, S.T.; Zhong, J.; Kang, Z. Metal-free efficient photocatalyst for stable visible water splitting via a two-electron pathway. *Science* **2015**, *347*, 970–974. [CrossRef] [PubMed]
165. Zhang, Z.; Long, J.; Yang, L.; Chen, W.; Dai, W.; Fu, X.; Wang, X. Organic semiconductor for artificial photosynthesis: Water splitting into hydrogen by a bioinspired C3N3S3 polymer under visible light irradiation. *Chem. Sci.* **2011**, *2*, 1826–1830. [CrossRef]
166. Liu, G.; Niu, P.; Yin, L.; Cheng, H.M. α-Sulfur crystals as a visible-light-active photocatalyst. *J. Am. Chem. Soc.* **2012**, *134*, 9070–9073. [CrossRef]
167. Wang, F.; Ng, W.K.H.; Jimmy, C.Y.; Zhu, H.; Li, C.; Zhang, L.; Li, Q. Red phosphorus: An elemental photocatalyst for hydrogen formation from water. *Appl. Catal. B Environ.* **2012**, *111*, 409–414. [CrossRef]
168. Zhu, M.; Sun, Z.; Fujitsuka, M.; Majima, T. Z-Scheme Photocatalytic Water Splitting on a 2D Heterostructure of Black Phosphorus/Bismuth Vanadate Using Visible Light. *Angew. Chem. Int. Ed.* **2018**, *57*, 2160–2164. [CrossRef] [PubMed]
169. Hou, Y.; Abrams, B.L.; Vesborg, P.C.; Björketun, M.E.; Herbst, K.; Bech, L.; Setti, A.M.; Damsgaard, C.D.; Pedersen, T.; Hansen, O.; et al. Bioinspired molecular co-catalysts bonded to a silicon photocathode for solar hydrogen evolution. *Nat. Mater.* **2011**, *10*, 434–438. [CrossRef]
170. Liu, J.; Wen, S.; Hou, Y.; Zuo, F.; Beran, G.J.O.; Feng, P. Boron Carbides as Efficient, Metal-Free, Visible-Light-Responsive Photocatalysts. *Angew. Chem. Int. Ed.* **2013**, *52*, 3241–3245. [CrossRef]
171. Chen, S.N.; Heeger, A.J.; Kiss, Z.; MacDiarmid, A.G.; Gau, S.C.; Peebles, D.L. Polyacetylene, (CH)x: Photoelectrochemical solar cell. *Appl. Phys. Lett.* **1980**, *36*, 96–98. [CrossRef]
172. Yamase, T.; Harada, H.; Ikawa, T.; Ikeda, S.; Shirakawa, H. A Photoelectrochemical Study of Polyacetylene, (CH)x. *Bull. Chem. Soc. Jpn.* **1981**, *54*, 2817–2818. [CrossRef]

173. Aizawa, M.; Watanabe, S.; Shinohara, H.; Shirakawa, H. Photodoping of polyacetylene films. *J. Chem. Soc. Chem. Commun.* **1985**, 62–63. [CrossRef]
174. Kaneko, M.; Okuzumi, K.; Yamada, A. Photocurrent generation by a liquid-junction poly (pyrrole) film. *J. Electroanal. Chem. Interfacial Electrochem.* **1985**, *183*, 407–410. [CrossRef]
175. Genies, E.M.; Lapkowski, M. Influence of light on the electrochemical behavior of polyaniline films. *Synth. Met.* **1988**, *24*, 69–76. [CrossRef]
176. Hursán, D.; Kormányos, A.; Rajeshwar, K.; Janáky, C. Polyaniline films photoelectrochemically reduce CO_2 to alcohols. *Chem. Commun.* **2016**, *52*, 8858–8861. [CrossRef] [PubMed]
177. Glenis, S.; Tourillon, G.; Garnier, F. Photoelectrochemical properties of thin films of polythiophene and derivatives: Doping level and structure effects. *Thin Solid Film.* **1984**, *122*, 9–17. [CrossRef]
178. El-Rashiedy, O.A.; Holdcroft, S. Photoelectrochemical properties of poly (3-alkylthiophene) films in aqueous solution. *J. Phys. Chem.* **1996**, *100*, 5481–5484. [CrossRef]
179. Suppes, G.; Ballard, E.; Holdcroft, S. Aqueous photocathode activity of regioregular poly (3-hexylthiophene). *Polym. Chem.* **2013**, *4*, 5345–5350. [CrossRef]
180. Schlettwein, D.; Jaeger, N.I. Identification of the Mechanism in the Photoelectrochemical Reduction of Oxygen on the Surface of a Molecular Semiconductor. *J. Phys. Chem.* **1993**, *97*, 3333–3337. [CrossRef]
181. Schlettwein, D.; Armstrong, N.R. Correlation of frontier orbital positions and conduction type of molecular semiconductors as derived from UPS in combination with electrical and photoelectrochemical experiments. *J. Phys. Chem.* **1994**, *98*, 11771–11779. [CrossRef]
182. Schlettwein, D.; Kaneko, M.; Yamada, A.; Wöhrle, D.; Jaeger, N.I. Light-induced dioxygen reduction at thin film electrodes of various porphyrins. *J. Phys. Chem.* **1991**, *95*, 1748–1755. [CrossRef]
183. Yanagi, H.; Kanbayashi, Y.; Schlettwein, D.; Woehrle, D.; Armstrong, N.R. Photoelectrochemical investigations on naphthalocyanine derivatives in thin films. *J. Phys. Chem.* **1994**, *98*, 4760–4766. [CrossRef]
184. Yanagida, S.; Kabumoto, A.; Mizumoto, K.; Pac, C.; Yoshino, K. Poly (p-phenylene)-catalysed photoreduction of water to hydrogen. *J. Chem. Soc. Chem. Commun.* **1991**, 474–475. [CrossRef]
185. Shibata, T.S.; Kabumoto, A.; Hiragami, T.S.; Ishitani, O.; Pac, C.; Yanagida, S. Novel visible-light-driven photocatalyst. Poly (p-phenylene)-catalyzed photoreductions of water, carbonyl compounds, and olefins. *J. Phys. Chem.* **1990**, *94*, 2068–2076. [CrossRef]
186. Matsuoka, S.; Fujii, H.; Yamada, T.; Pac, C.; Ishida, A.; Takamuku, S.; Kusaba, M.; Nakashima, N.; Yanagida, S. Photocatalysis of oligo (p-phenylenes): Photoreductive production of hydrogen and ethanol in aqueous triethylamine. *J. Phys. Chem.* **1991**, *95*, 5802–5808. [CrossRef]
187. Maruo, K.; Yamada, K.; Wada, Y.; Yanagida, S. Visible-light induced photocatalysis of partially fluorinated poly (p-phenylene) and related linear phenylene derivatives. *Bull. Chem. Soc. Jpn.* **1993**, *66*, 1053–1064. [CrossRef]
188. Li, S.; Ye, L.; Zhao, W.; Yan, H.; Yang, B.; Liu, D.; Li, W.; Ade, H.; Hou, J. A Wide Band Gap Polymer with a Deep Highest Occupied Molecular Orbital Level Enables 14.2% Efficiency in Polymer Solar Cells. *J. Am. Chem. Soc.* **2018**, *140*, 7159–7167. [CrossRef]
189. Green, M.A.; Emery, K.; Hishikawa, Y.; Warta, W.; Dunlop, E.D. Solar cell efficiency tables (version 46). *Prog. Photovoltaics Res. Appl.* **2015**, *23*, 1–9. [CrossRef]
190. Thompson, B.C.; Fréchet, J.M. Polymer–fullerene composite solar cells. *Angew. Chem. Int. Ed.* **2008**, *47*, 58–77. [CrossRef]
191. Günes, S.; Neugebauer, H.; Sariciftci, N.S. Conjugated polymer-based organic solar cells. *Chem. Rev.* **2007**, *107*, 1324–1338. [CrossRef]
192. Matsuo, Y.; Sato, Y.; Niinomi, T.; Soga, I.; Tanaka, H.; Nakamura, E. Columnar structure in bulk heterojunction in solution-processable three-layered pin organic photovoltaic devices using tetrabenzoporphyrin precursor and silylmethyl fullerene. *J. Am. Chem. Soc.* **2009**, *131*, 16048–16050. [CrossRef]
193. Hiramoto, M.; Fujiwara, H.; Yokoyama, M. Three-layered organic solar cell with a photoactive interlayer of codeposited pigments. *Appl. Phys. Lett.* **1991**, *58*, 1062–1064. [CrossRef]
194. Peumans, P.; Uchida, S.; Forrest, S.R. Efficient bulk heterojunction photovoltaic cells using small-molecular-weight organic thin films. *Nature* **2003**, *425*, 158–162. [CrossRef] [PubMed]
195. Sariciftci, N.S.; Smilowitz, L.; Heeger, A.J.; Wudl, F. Photoinduced electron transfer from a conducting polymer to buckminsterfullerene. *Science* **1992**, *258*, 1474–1476. [CrossRef] [PubMed]
196. Tang, C.W. Two-layer organic photovoltaic cell. *Appl. Phys. Lett.* **1986**, *48*, 183–185. [CrossRef]
197. Abe, T.; Ichinohe, H.; Kakuta, S.; Nagai, K. Organic photoanode of fullerene/phthalocyanine working in the water phase with respect to preparation methods of the bilayer film. *Jpn. J. Appl. Phys.* **2010**, *49*, 015101. [CrossRef]
198. Abe, T.; Tanno, Y.; Ebina, T.; Miyakushi, S.; Nagai, K. Enhanced photoanodic output at an organic p/n bilayer in the water phase by means of the formation of whiskered phthalocyanine. *ACS Appl. Mater. Interfaces* **2013**, *5*, 1248–1253. [CrossRef]
199. Ahmad, M.F.; Abe, T.; Musgrave, C.S.; Nagai, K. Study of Co-deposition Photoelectrode of Perylene Derivative and Phthalocyanine in Comparison with Its Bilayer Focusing on Charge Transfer Complex and Kinetic Analysis. *Electrochemistry* **2018**, 235–242. [CrossRef]
200. Ahmad, M.F.; Suzuki, M.; Abe, T.; Nagai, K. Enhanced oxidation power in photoelectrocatalysis based on a micrometer-localized positive potential in a terrace hetero p–n junction. *NPG Asia Mater.* **2018**, *10*, 630–641. [CrossRef]

201. Abe, T.; Ichikawa, M.; Hikage, T.; Kakuta, S.; Nagai, K. Relationship between the morphology of poly (3-hexylthiophene)/methanofullerene composite and its photoelectrode characteristics in the water phase. *Chem. Phys. Lett.* **2012**, *549*, 77–81. [CrossRef]
202. Nagai, K.; Kuwabara, T.; Ahmad, M.-A.; Nakano, M.; Karakawa, M.; Taima, T.; Takahashi, K. High performance photoanodic catalyst prepared from an active organic photovoltaic cell -high potential gain from visible light. *Chem. Commun.* **2019**, *55*, 12491–12494. [CrossRef]
203. Nagai, K.; Abe, T. Full-Spectrum-Visible-Light Photocatalyst Based on the Active Layer of Organic Solar Cell-Towards Water Splitting and Volatile Molecule Degradation. *Kobunshi Ronbunshu* **2013**, *7*, 459–475. [CrossRef]
204. Abe, T.; Nagai, K.; Kabutomori, S.; Kaneko, M.; Tajiri, A.; Norimatsu, T. An Organic Photoelectrode Working in the Water Phase: Visible-Light-Induced Dioxygen Evolution by a Perylene Derivative/Cobalt Phthalocyanine Bilayer. *Angew. Chem. Int. Ed.* **2006**, *45*, 2778–2781. [CrossRef] [PubMed]
205. Abe, T.; Nagai, K.; Ogiwara, T.; Ogasawara, S.; Kaneko, M.; Tajiri, A.; Norimatsu, T. Wide visible light-induced dioxygen evolution at an organic photoanode coated with a noble metal oxide catalyst. *J. Electroanal. Chem.* **2006**, *587*, 127–132. [CrossRef]
206. Yang, S.; Fan, L.; Yang, S. Significantly enhanced photocurrent efficiency of a poly (3-hexylthiophene) photoelectrochemical device by doping with the endohedral metallofullerene Dy@ C82. *Chem. Phys. Lett.* **2004**, *388*, 253–258. [CrossRef]
207. Bornoz, P.; Prévot, M.S.; Yu, X.; Guijarro, N.; Sivula, K. Direct light-driven water oxidation by a ladder-type conjugated polymer photoanode. *J. Am. Chem. Soc.* **2015**, *137*, 15338–15341. [CrossRef] [PubMed]
208. Lanzarini, E.; Antognazza, M.R.; Biso, M.; Ansaldo, A.; Laudato, L.; Bruno, P.; Metrangolo, P.; Resnati, G.; Ricci, D.; Lanzani, G. Polymer-based photocatalytic hydrogen generation. *J. Phys. Chem. C* **2012**, *116*, 10944–10949. [CrossRef]
209. Chu, S.; Li, W.; Yan, Y.; Hamann, T.; Shih, I.; Wang, D.; Mi, Z. Roadmap on solar water splitting: Current status and future prospects. *Nano Futures* **2017**, *1*, 022001. [CrossRef]
210. Mezzetti, A.; Fumagalli, F.; Alfano, A.; Iadicicco, D.; Antognazza, M.R.; di Fonzo, F. Stable hybrid organic/inorganic photocathodes for hydrogen evolution with amorphous WO 3 hole selective contacts. *Faraday Discuss.* **2017**, *198*, 433–448. [CrossRef]
211. Wang, L.; Yan, D.; Shaffer, D.W.; Ye, X.; Layne, B.H.; Concepcion, J.J.; Liu, M.; Nam, C.Y. Improved Stability and Performance of Visible Photoelectrochemical Water Splitting on Solution-Processed Organic Semiconductor Thin Films by Ultrathin Metal Oxide Passivation. *Chem. Mater.* **2018**, *30*, 324–335. [CrossRef]
212. Francàs, L.; Burns, E.; Steier, L.; Cha, H.; Solà-Hernández, L.; Li, X.; Tuladhar, P.S.; Bofill, R.; Garcia-Anton, J.; Sala, X.; et al. Rational design of a neutral pH functional and stable organic photocathode. *Chem. Commun.* **2018**, *54*, 5732–5735. [CrossRef]
213. Sun, T.; Song, J.; Jia, J.; Li, X.; Sun, X. Real roles of perylenetetracarboxylic diimide for enhancing photocatalytic H2-production. *Nano Energy* **2016**, *26*, 83–89. [CrossRef]
214. Li, J.X.; Li, Z.J.; Ye, C.; Li, X.B.; Zhan, F.; Fan, X.B.; Li, J.; Chen, B.; Tao, Y.; Tung, C.H.; et al. Visible light-induced photochemical oxygen evolution from water by 3, 4, 9, 10-perylenetetracarboxylic dianhydride nanorods as an n-type organic semiconductor. *Catal. Sci. Technol.* **2016**, *6*, 672–676. [CrossRef]
215. Kirner, J.T.; Stracke, J.J.; Gregg, B.A.; Finke, R.G. Visible-light-assisted photoelectrochemical water oxidation by thin films of a phosphonate-functionalized perylene diimide plus CoO x cocatalyst. *ACS Appl. Mater. Interfaces* **2014**, *6*, 13367–13377. [CrossRef] [PubMed]
216. Abe, T.; Chiba, J.; Ishidoya, M.; Nagai, K. Organophotocatalysis system of p/n bilayers for wide visible-light-induced molecular hydrogen evolution. *RSC Adv.* **2012**, *2*, 7992–7996. [CrossRef]
217. Abe, T.; Fukui, K.; Kawai, Y.; Nagai, K.; Kato, H. A water splitting system using an organo-photocathode and titanium dioxide photoanode capable of bias-free H_2 and O_2 evolution. *Chem. Commun.* **2016**, *52*, 7735–7737. [CrossRef]
218. Abe, T.; Taira, N.; Tanno, Y.; Kikuchi, Y.; Nagai, K. Decomposition of hydrazine by an organic fullerene–phthalocyanine p–n bilayer photocatalysis system over the entire visible-light region. *Chem. Commun.* **2014**, *50*, 1950–1952. [CrossRef]
219. Abe, T.; Tanno, Y.; Taira, N.; Nagai, K. Efficient organo-photocatalysis system of an n-type perylene derivative/p-type cobalt phthalocyanine bilayer for the production of molecular hydrogen from hydrazine. *RSC Adv.* **2015**, *5*, 46325–46329. [CrossRef]
220. Kawai, Y.; Nagai, K.; Abe, T. A visible-light-induced photoelectrochemical water-splitting system featuring an organo-photocathode along with a tungsten oxide photoanode. *RSC Adv.* **2017**, *7*, 34694–34698. [CrossRef]
221. Bourgeteau, T.; Tondelier, D.; Geffroy, B.; Brisse, R.; Laberty-Robert, C.; Campidelli, S.; Bettignies, R.D.; Artero, V.; Palacin, S.; Jousselme, B. A H2-evolving photocathode based on direct sensitization of MoS3 with an organic photovoltaic cell. *Energy Environ. Sci.* **2013**, *6*, 2706–2713. [CrossRef]
222. Tran, P.D.; Tran, T.V.; Orio, M.; Torelli, S.; Truong, Q.D.; Nayuki, K.; Sasaki, Y.; Chiam, S.Y.; Yi, R.; Honma, I.; et al. Coordination polymer structure and revisited hydrogen evolution catalytic mechanism for amorphous molybdenum sulfide. *Nat. Mater.* **2016**, *15*, 640. [CrossRef]
223. Haro, M.; Solis, C.; Molina, G.; Otero, L.; Bisquert, J.; Gimenez, S.; Guerrero, A. Toward stable solar hydrogen generation using organic photoelectrochemical cells. *J. Phys. Chem. C* **2015**, *119*, 6488–6494. [CrossRef]
224. Steier, L.; Bellani, S.; Rojas, H.C.; Pan, L.; Laitinen, M.; Sajavaara, T.; Fonzo, F.D.; Grätzel, M.; Antognazza, M.R.; Mayer, M.T. Stabilizing organic photocathodes by low-temperature atomic layer deposition of TiO_2. *Sustain. Energy Fuels* **2017**, *1*, 1915–1920. [CrossRef]
225. Bourgeteau, T.; Tondelier, D.; Geffroy, B.; Brisse, R.; Cornut, R.; Artero, V.; Jousselme, B. Enhancing the Performances of P3HT: PCBM–MoS3-Based H2-Evolving Photocathodes with Interfacial Layers. *ACS Appl. Mater. Interfaces* **2015**, *7*, 16395–16403. [CrossRef] [PubMed]

226. Bourgeteau, T.; Tondelier, D.; Geffroy, B.; Brisse, R.; Campidelli, S.; Cornut, R.; Jousselme, B. All solution-processed organic photocathodes with increased efficiency and stability via the tuning of the hole-extracting layer. *J. Mater. Chem. A* **2016**, *4*, 4831–4839. [CrossRef]
227. Bellani, S.; Antognazza, M.R.; Bonaccorso, F. Carbon-Based Photocathode Materials for Solar Hydrogen Production. *Adv. Mater.* **2018**, 1801446. [CrossRef] [PubMed]
228. Fumagalli, F.; Bellani, S.; Schreier, M.; Leonardi, S.; Rojas, H.C.; Ghadirzadeh, A.; Tullii, G.; Savoini, A.; Marra, G.; Meda, L.; et al. Hybrid organic-inorganic H2-evolving photocathodes: Understanding the route towards high performance organic photoelectrochemical water splitting. *J. Mater. Chem. A* **2016**, *4*, 2178–2187. [CrossRef]
229. Belarb, E.; Blas-Ferrando, V.M.; Haro, M.; Maghraoui-Meherzi, H.; Gimenez, S. Electropolymerized polyaniline: A promising hole selective contact in organic photoelectrochemical cells. *Chem. Eng. Sci.* **2016**, *154*, 143–149. [CrossRef]
230. Rojas, H.C.; Bellani, S.; Fumagalli, F.; Tullii, G.; Leonardi, S.; Mayer, M.T.; Schriever, M.; Grätzel, M.; Lanzani, G.; Fonzo, F.D.; et al. Polymer-based photocathodes with a solution-processable cuprous iodide anode layer and a polyethyleneimine protective coating. *Energy Environ. Sci.* **2016**, *9*, 3710–3723. [CrossRef]
231. Morozan, A.; Bourgeteau, T.; Tondelier, D.; Geffroy, B.; Jousselme, B.; Artero, V. Noble metal-free hydrogen-evolving photocathodes based on small molecule organic semiconductors. *Nanotechnology* **2016**, *27*, 355401. [CrossRef]
232. Gao, Y.; Le Corre, V.M.; Gaïtis, A.; Neophytou, M.; Hamid, M.A.; Takanabe, K.; Beaujuge, P.M. Homo-Tandem Polymer Solar Cells with VOC > 1.8 V for Efficient PV-Driven Water Splitting. *Adv. Mater.* **2016**, *28*, 3366–3373. [CrossRef]
233. You, J.; Chen, C.C.; Hong, Z.; Yoshimura, K.; Ohya, K.; Xu, R.; Ye, S.; Gao, J.; Li, G.; Yang, Y. 10.2% power conversion efficiency polymer tandem solar cells consisting of two identical sub-cells. *Adv. Mater.* **2013**, *25*, 3973–3978. [CrossRef] [PubMed]
234. Esiner, S.; van Eersel, H.; Wienk, M.M.; Janssen, R.A. Triple junction polymer solar cells for photoelectrochemical water splitting. *Adv. Mater.* **2013**, *25*, 2932–2936. [CrossRef] [PubMed]
235. Esiner, S.; van Pruissen, G.W.; Wienk, M.M.; Janssen, R.A. Optimized light-driven electrochemical water splitting with tandem polymer solar cells. *J. Mater. Chem. A* **2016**, *4*, 5107–5114. [CrossRef]
236. Esiner, S.; Willems, R.E.; Furlan, A.; Li, W.; Wienk, M.M.; Janssen, R.A. Photoelectrochemical water splitting in an organic artificial leaf. *J. Mater. Chem.* **2015**, *3*, 23936–23945. [CrossRef]
237. Chen, S.; Zhang, G.; Liu, J.; Yao, H.; Zhang, J.; Ma, T.; Yan, H. An All-Solution Processed Recombination Layer with Mild Post-Treatment Enabling Efficient Homo-Tandem Non-fullerene Organic Solar Cells. *Adv. Mater.* **2017**, *29*, 1604231. [CrossRef]
238. Esiner, S.; van Eersel, H.; van Pruissen, G.W.; Turbiez, M.; Wienk, M.M.; Janssen, R.A. Water splitting with series-connected polymer solar cells. *ACS Appl. Mater. Interfaces* **2016**, *8*, 26972–26981. [CrossRef]
239. Windle, C.D.; Chandrasekaran, S.; Kumagai, H.; Sahara, G.; Nagai, K.; Abe, T.; Chavarot-Kerlidou, M.; Ishitani, O.; Artero, V. Molecular Design of Photocathode Materials for Hydrogen Evolution and Carbon Dioxide Reduction, Chapter 10. In *Molecular Technology: Energy Innovation*; Yamamoto, H., Kato, T., Eds.; Wiley: Hoboken, NJ, USA, 2018; pp. 251–286. ISBN 9783527341.
240. Li, C.; Liu, M.; Pschirer, N.G.; Baumgarten, M.; Mullen, K. Polyphenylene-based materials for organic photovoltaics. *Chem. Rev.* **2010**, *110*, 6817–6855. [CrossRef]
241. Steier, L.; Holliday, S. A bright outlook on organic photoelectrochemical cells for water splitting. *J. Mater. Chem. A* **2018**, *6*, 21809–21826. [CrossRef]
242. Kirner, J.T.; Finke, R.G. Water-oxidation photoanodes using organic light-harvesting materials: A review. *J. Mater. Chem. A* **2017**, *5*, 19560–19592. [CrossRef]
243. Rudolf, M.; Kirner, S.V.; Guldi, D.M. A multicomponent molecular approach to artificial photosynthesis–the role of fullerenes and endohedral metallofullerenes. *Chem. Soc. Rev.* **2016**, *45*, 612–630. [CrossRef]
244. Queyriaux, N.; Kaeffer, N.; Morozan, A.; Chavarot-Kerlidou, M.; Artero, V. Molecular cathode and photocathode materials for hydrogen evolution in photoelectrochemical devices. *J. Photochem. Photobiol. C Photochem. Rev.* **2015**, *25*, 90–105. [CrossRef]
245. Artero, V.; Chavarot-Kerlidou, M.; Fontecave, M. Splitting water with cobalt. *Angew. Chem. Int. Ed.* **2011**, *50*, 7238–7266. [CrossRef] [PubMed]
246. Wen, J.; Xie, J.; Chen, X.; Li, X. A review on g-C_3N_4-based photocatalysts. *Appl. Surf. Sci.* **2017**, *391*, 72–123. [CrossRef]
247. Chen, Y.Z.; Li, W.H.; Li, L.; Wang, L.N. Progress in organic photocatalysts. *Rare Met.* **2018**, *37*, 1–12. [CrossRef]
248. Sprick, R.S.; Bonillo, B.; Sachs, M.; Clowes, R.; Durrant, J.R.; Adams, D.J.; Cooper, A.I. Extended conjugated microporous polymers for photocatalytic hydrogen evolution from water. *Chem. Commun.* **2016**, *52*, 10008–10011. [CrossRef]
249. Sick, T.; Hufnagel, A.G.; Kampmann, J.; Kondofersky, I.; Calik, M.; Rotter, J.M.; Böhm, D. Oriented films of conjugated 2D covalent organic frameworks as photocathodes for water splitting. *J. Am. Chem. Soc.* **2018**, *140*, 2085–2092. [CrossRef]
250. Kumaravel, V.; Bartlett, J.; Pillai, S.C. Photoelectrochemical conversion of carbon dioxide (CO_2) into fuels and value-added products. *ACS Energy Lett.* **2020**, *5*, 486–519. [CrossRef]
251. Galan-Mascaros, J.R. Photoelectrochemical solar fuels from carbon dioxide, water and sunlight. *Catal. Sci. Technol.* **2020**, *10*, 1967–1974. [CrossRef]
252. Montoya, J.H.; Seitz, L.C.; Chakthranont, P.; Vojvodic, A.; Jaramillo, T.F.; Nørskov, J.K. Materials for solar fuels and chemicals. *Nat. Mater.* **2017**, *16*, 70–81. [CrossRef]
253. Kalamaras, E.; Maroto-Valer, M.M.; Shao, M.; Xuan, J.; Wang, H. Solar carbon fuel via photoelectrochemistry. *Catal. Today* **2018**, *317*, 56–75. [CrossRef]